

## Designing bioresponsive nanomaterials for intracellular self-assembly

Sarah Chagri , David Y. W. Ng ✉ and Tanja Weil ✉

**Abstract** | Supramolecular assemblies are essential components of living organisms. Cellular scaffolds, such as the cytoskeleton or the cell membrane, are formed via secondary interactions between proteins or lipids and direct biological processes such as metabolism, proliferation and transport. Inspired by nature's evolution of function through structure formation, a range of synthetic nanomaterials has been developed in the past decade, with the goal of creating non-natural supramolecular assemblies inside living mammalian cells. Given the intricacy of biological pathways and the compartmentalization of the cell, different strategies can be employed to control the assembly formation within the highly crowded, dynamic cellular environment. In this Review, we highlight emerging molecular design concepts aimed at creating precursors that respond to endogenous stimuli to build nanostructures within the cell. We describe the underlying reaction mechanisms that can provide spatial and temporal control over the subcellular formation of synthetic nanostructures. Showcasing recent advances in the development of bioresponsive nanomaterials for intracellular self-assembly, we also discuss their impact on cellular function and the challenges associated with establishing structure–bioactivity relationships, as well as their relevance for the discovery of novel drugs and imaging agents, to address the shortfall of current solutions to pressing health issues.

In nature, the formation of functional structures through the assembly of smaller units can be observed over several structural hierarchies at the macroscopic, microscopic and nanoscopic scales. While spiderwebs are tangible examples of natural constructs built for specific function, eukaryotic cells reveal that similar phenomena also exist on a molecular level: for instance, the cytoskeleton is made from various dynamic protein assemblies that form intricate networks inside the cell, ensuring cellular stability, motility and division<sup>1</sup>. Mimicking these naturally occurring structures by integrating synthetic self-assembled nanostructures in a biological context is an important milestone in supramolecular chemistry, as these systems expand the boundaries of both nanomedicine and synthetic biology. Additionally, the bottom-up approach of creating non-natural assemblies inside cells could help elucidate molecular mechanisms of naturally occurring cellular processes and provide the foundation to unravel the origin of life<sup>2</sup>.

Regarding the potential of synthetic supramolecular nanostructures for therapeutic applications<sup>3</sup>, a major appeal is the circumvention of limitations that small molecule drugs face, such as drug resistance in cancer cells<sup>4</sup>. In contrast to small molecules, systems

capable of intracellular self-assembly can form large aggregates inside cells, which forces their accumulation at the target site<sup>5</sup>, resulting in improved pharmacokinetics. Additionally, the process of self-assembly can cause mechanical stress due to the disruption of cellular structures, thus, triggering cell death<sup>6</sup>. By instilling bioresponsiveness — in which molecules react to physiological cues — in the design of the assembly precursor, its conversion to an active self-assembling monomer can be precisely tailored to a specific nanoenvironment or microenvironment in the cell. Targeted intracellular stimuli include those that have been widely exploited in state-of-the-art prodrugs and delivery systems, such as pH (REFS<sup>7–11</sup>), redox<sup>6,12–15</sup> or enzymes<sup>16–22</sup>, in which the respective stimulus is often characteristic for a certain subcellular location (FIG. 1). As the considerations to program nanostructure formation within cells are multifaceted, we aim to streamline the design concepts to create greater accessibility and understanding for the scientific community. In this Review, we showcase successful molecular design principles to control the assembly of functional nanostructures within mammalian cells, which are triggered by endogenous stimuli. Assemblies in bacteria are excluded, as the conditions of transport

Max Planck Institute for  
Polymer Research, Mainz,  
Germany.

✉e-mail: david.ng@  
mpip-mainz.mpg.de;  
weil@mpip-mainz.mpg.de  
[https://doi.org/10.1038/  
s41570-022-00373-x](https://doi.org/10.1038/s41570-022-00373-x)

and the available physiological stimuli are different, thus, requiring a distinct set of molecular considerations<sup>23,24</sup>. Recent advances in this field have been summarized in other review articles<sup>25,26</sup>.

Furthermore, while other reviews on synthetic assemblies inside mammalian cells have focused more on potential biological applications for bioimaging or chemotherapy<sup>27–30</sup>, our main goal is to examine the underlying design principles, considerations and challenges of creating bioresponsive precursors for the formation of supramolecular nanostructures, with an emphasis on the spatiotemporal control over the intracellular assembly.

### Cellular compartments as reaction vessels

The eukaryotic cell is an intricate machinery made of lipids, proteins and genetic material, all forming supra-molecular structures in an aqueous environment, while dynamic chemical crosstalk between organelles and the extracellular space governs internal processes<sup>31</sup>. The living cell is a non-equilibrium system characterized by compartmentalization and the energy-dependent maintenance of concentration gradients that are essential for proliferation and function<sup>32</sup>. As cellular compartments fulfil different tasks within the cell, they often provide distinct (bio)chemical environments, such as a certain

pH, redox environment, level of molecular crowding or the presence of specific enzymes<sup>31</sup> (FIG. 1).

From a chemist's perspective, cellular compartments with their distinct characteristics are analogous to a system of interconnected reaction vessels, each offering different reaction conditions for chemical transformations. When designing synthetic materials for intracellular self-assembly, a knowledge of cell biology is essential to understand and exploit structure–(bio)activity relationships. In terms of molecular design, this means carefully choosing the respective functional groups and other elements, such as enzyme recognition sites, to implement selectivity towards a biological or chemical stimulus associated with a target subcellular location. For example, the decrease in pH associated with the endocytic pathway can be exploited by using pH-sensitive materials that can undergo supramolecular transformations inside the acidic endosomal or lysosomal environments due to protonation or isomerization<sup>7–11</sup>. Similarly, the reducing medium of the cytosol can induce the chemical conversion of reduction-sensitive precursors into active monomers upon cell entry<sup>12,15</sup>, while the higher concentration of reactive oxygen species (ROS) near the mitochondria can lead to oxidation-driven self-assembly in the vicinity of these organelles<sup>14</sup>.

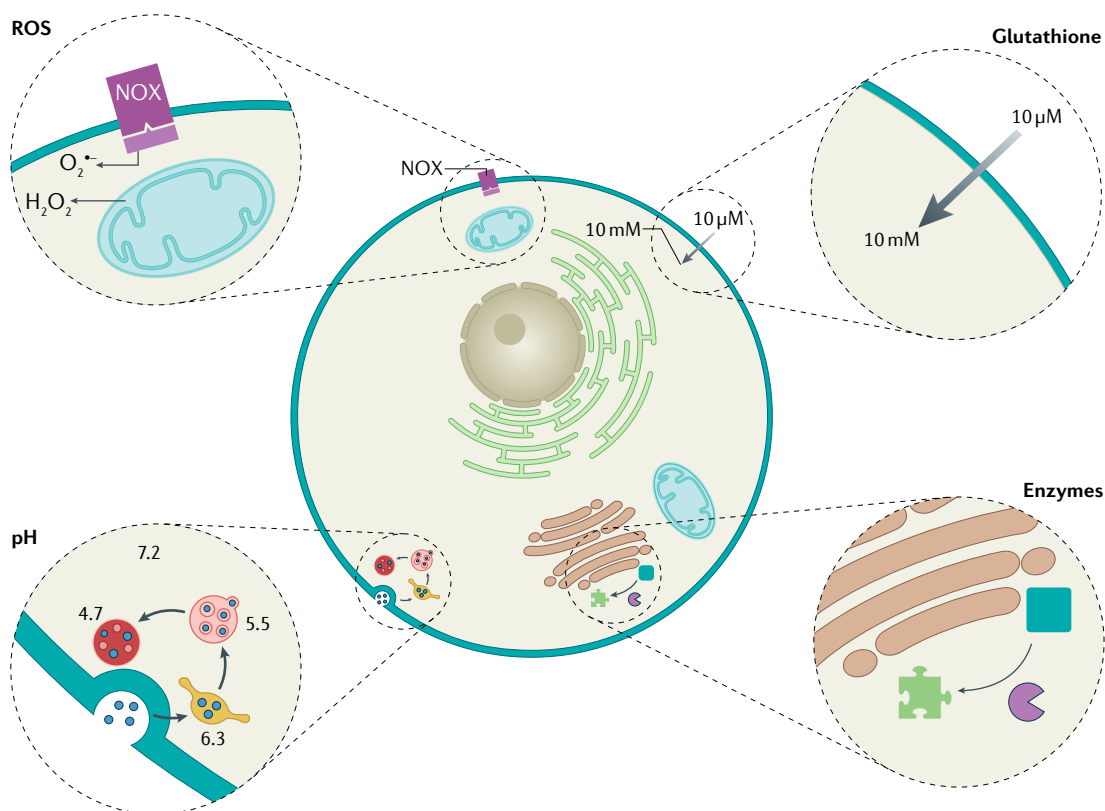


**Fig. 1 | The eukaryotic cell and its compartments as interconnected reaction vessels.** The conditions for chemical transformation of bioresponsive nanomaterials in terms of pH, redox environment and enzyme catalysis differ widely, depending on the subcellular location. While reactive oxygen species (ROS) are mainly generated in the mitochondria<sup>103</sup>, as well as, to a lesser degree, by the membrane-bound NADPH oxidase (NOX)<sup>96</sup>, the cellular reducing agent glutathione is present in high concentration (10 mM) throughout the cytosol<sup>155</sup>. During the endocytic pathway, the pH inside the vesicles decreases significantly from 6.3 in the early endosomes to 5.5 in the late endosomes to 4.7 in the lysosomes, whereas the cytosolic pH is typically neutral, at around 7.2 (REF.<sup>83</sup>). The localization of enzymes within the cells depends on their respective biocatalytic function, meaning that they are often associated with specific organelles.

Besides the influence of different reaction conditions associated with intracellular location, the cell type also affects the efficiency of chemical transformations, as cells from different tissues have evolved to behave in specific ways that contribute to the survival of the whole organism. For example, liver cells, which are in charge of detoxification, display a comparatively high cytosolic concentration of glutathione, a cellular antioxidant and nucleophile essential for scavenging harmful electrophilic compounds and ROS<sup>33</sup>. Moreover, the gene expression profile of cells also varies depending on the tissue, which includes the expression levels of certain enzymes, such as proteases, that catalyse biochemical transformations.

Alterations in the genetic code can cause cells to cease following expected patterns and instead start displaying an opportunistic, self-serving behaviour targeted at sustained growth and evasion of cell death<sup>34</sup>. These cancerous cells can emerge from different tissues and often show an upregulation of pro-proliferative and pro-angiogenic factors, as well as an elevated cellular metabolism<sup>35</sup>. While cancer cells are not uniform in their biological and chemical characteristics, there are some common properties of aggressively growing cancers, for example: the acidification of the tumour extracellular microenvironment because of their enhanced glycolytic rate, a tendency to develop low oxygen level in tissue, called hypoxia, due to limited oxygen supply inside the tumour and the overexpression of certain proteases that aid cell invasion and metastasis<sup>34</sup>. Regarding the great challenges associated with drug-resistant cancers, upregulated efflux pumps, such as P-glycoprotein<sup>36</sup>, and elevated glutathione levels in the cytosol<sup>37</sup> play critical roles in treatment failure due to drug inactivation and efficient removal. Therefore, in addition to using targeting moieties that are recognized by specific cell surface receptors, the aforementioned distinct features of cancerous cells can facilitate the design of novel cancer-specific drugs or imaging agents with less toxic side effects on healthy cells or tissue<sup>38</sup>. Consequently, these considerations are also relevant for controlling the bioresponsive formation of synthetic nanostructures within cancer cells, which offers entirely new avenues to potentially revolutionize bioimaging and cancer therapy.

### Nanomaterials for intracellular self-assembly

Creating synthetic supramolecular assemblies in a biological environment requires molecular design strategies that fulfil necessary criteria regarding biocompatibility, environmental responsiveness and the propensity for self-assembly within crowded and complex environments. For instance, the assembly precursor must enter cells without premature disruption of cellular functions or causing cell death, since a lack of biocompatibility at this stage would impede the formation of nanostructures at the desired cellular location. Efficient cell uptake of the precursor can be achieved by including structural elements that promote cell entry in the molecular design, such as cell-penetrating peptides (CPPs)<sup>68</sup> or ligands of certain cell surface receptors<sup>5,39,40</sup>. CPPs comprise 40 or less amino acids and they can be conjugated covalently or non-covalently to cargo to facilitate their delivery into

the cell<sup>41,42</sup>. Besides direct translocation into the cytosol as a result of attractive electrostatic interaction with the negatively charged plasma membrane<sup>42</sup>, CPPs and their conjugates can also be internalized through various endocytic pathways<sup>43</sup>. While some aspects of the cell uptake mechanisms remain elusive, prominent examples of cationic CPPs such as the HIV-derived peptide transactivator of transcription or polyarginine peptides have been shown to enter cells through a variety of pathways, depending on the cell type and the conjugated cargo<sup>44–46</sup>. However, using CPPs for intracellular delivery of assembly precursors can come with the limitation of lacking cell selectivity, whereas the introduction of certain ligands for receptor-mediated endocytosis can tailor the system towards a more targeted effect<sup>5,39,40</sup>. For example, the tripeptide RGD serves as a recognition motif for integrin cell surface receptors, such as  $\alpha v \beta 3$ , which are overexpressed in many cancer cells<sup>47</sup>. Therefore, assembly precursors that are modified with the linear or cyclic version of the targeting peptide have been employed for cancer-specific targeting both in vitro<sup>10,39,40</sup> and in vivo<sup>5</sup>.

For the in vivo application of nanomaterials for intracellular structure formation, achieving tissue selectivity by active or passive targeting is one of the key objectives. Besides the use of tumour-specific recognition motifs<sup>48</sup>, the so-called enhanced permeability and retention effect in solid tumours with high vascular density and high endothelial permeability<sup>49</sup> contributes to the passive accumulation of macromolecular precursors at the desired location<sup>12</sup>. In general, the administration of compounds for intracellular self-assembly comes with similar challenges in terms of pharmacokinetics and immunogenicity as observed for small molecule drugs<sup>48</sup>; however, these pro-assembling systems can possess greater selectivity and avoid affecting healthy cells. This is due to the bioresponsive mode of action of the assembly precursors, which require the presence of a specific stimulus inside the cells and confines the assembly formation to the intracellular space<sup>48,50</sup>.

Within the cell, the activated self-assembling monomer resulting from intracellular chemical conversion needs to display a critical aggregation concentration that is sufficiently low for self-assembly under physiological conditions, which is usually in the micromolar range<sup>9,51</sup>. The critical aggregation concentration of the active monomer is determined by the self-assembly propensity of the material, which is based on attractive intermolecular interactions. Since the intracellular environment displays a high degree of macromolecular crowding due to, for example, soluble proteins, densely packed filamentous structures and phase-separated components, this increases diffusional obstacles and further enhances the inherent aggregation tendency of the monomers<sup>52,53</sup>. However, this abundance of biomacromolecules with reactive groups, such as proteins with surface-exposed cysteines<sup>54</sup>, as well as other ubiquitous molecules such as glutathione<sup>55</sup> or ROS<sup>56</sup>, mandates the need for biorthogonality of the assembly precursor to prevent unwanted interactions. This biorthogonality is also important for achieving spatial control over the subcellular structure formation, which can additionally be aided by introducing

**Pro-proliferative**  
Promoting cellular reproduction.

**Pro-angiogenic**  
Promoting blood vessel formation.

**Efflux pumps**  
Membrane proteins responsible for the export of substances from the cell.

**J-aggregates**

Aggregates of fluorescent dyes characterized by a narrow absorption band that is shifted to a longer wavelength (bathochromic shift) in comparison with the monomer and a small Stokes shift with a narrow band.

**Luminogens**

Compounds that exhibit an increase in luminescence or fluorescence upon aggregation instead of self-quenching.

organelle-specific targeting groups to the precursor that ferry the pro-assembling material through the cellular environment to the desired compartment<sup>57</sup>.

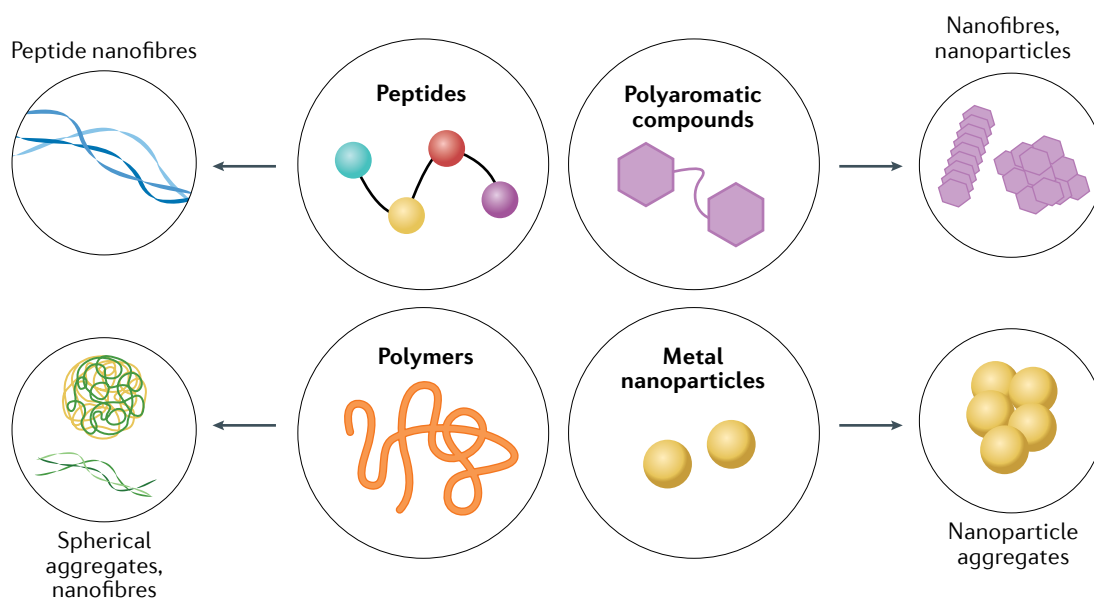
Generally, there are four material classes that are commonly used for intracellular self-assembly: peptides, polyaromatic compounds, polymers and metal nanoparticles (FIG. 2). While there are only a few examples of polymers<sup>14,58</sup> or metal nanoparticles<sup>59–61</sup> that have shown intracellular structure formation, many peptide-based and polyaromatic materials readily undergo stimuli-responsive self-assembly in cellular environments, providing new perspectives for diagnostic or therapeutic applications.

Peptides, more specifically,  $\beta$ -sheet forming so-called amyloid-like peptides, constitute one of the most popular scaffold materials: they are characterized by amphiphilicity caused by an alternating sequence pattern of polar and nonpolar amino acids, which supports the intermolecular hydrogen bonding necessary for adopting  $\beta$ -sheet secondary structures<sup>62</sup>. Moreover, they usually display a high content of aromatic amino acids, such as phenylalanine, required for self-assembly due to  $\pi$ - $\pi$  stacking and van der Waals interactions<sup>53,63</sup>. Often, an aromatic moiety or fluorophore at the amino terminus further adds to their  $\pi$ - $\pi$  stacking tendency, supporting their assembly into stable nanostructures<sup>62</sup>. For instance, certain peptides can form ordered  $\beta$ -sheet-rich nanofibres of a few nanometres in width and micrometres in length that show similarities to naturally occurring  $\beta$ -amyloid aggregates present in various neurodegenerative illnesses, such as Alzheimer disease<sup>62</sup>. Amphiphilic peptide conjugates are another subcategory of peptide-based nanomaterials consisting

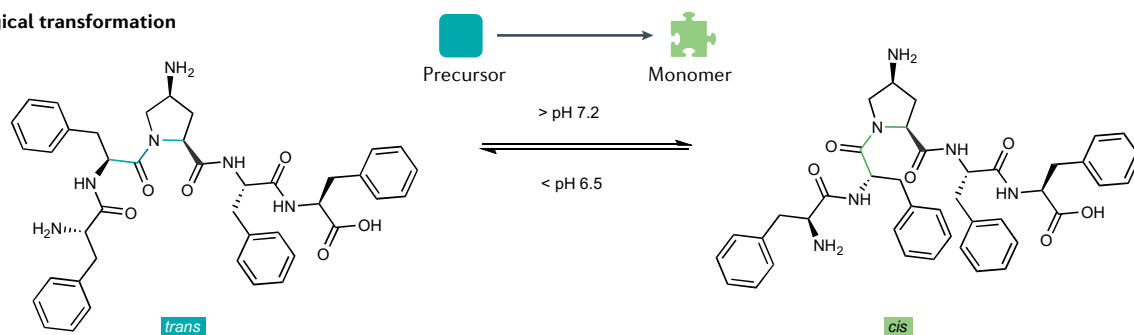
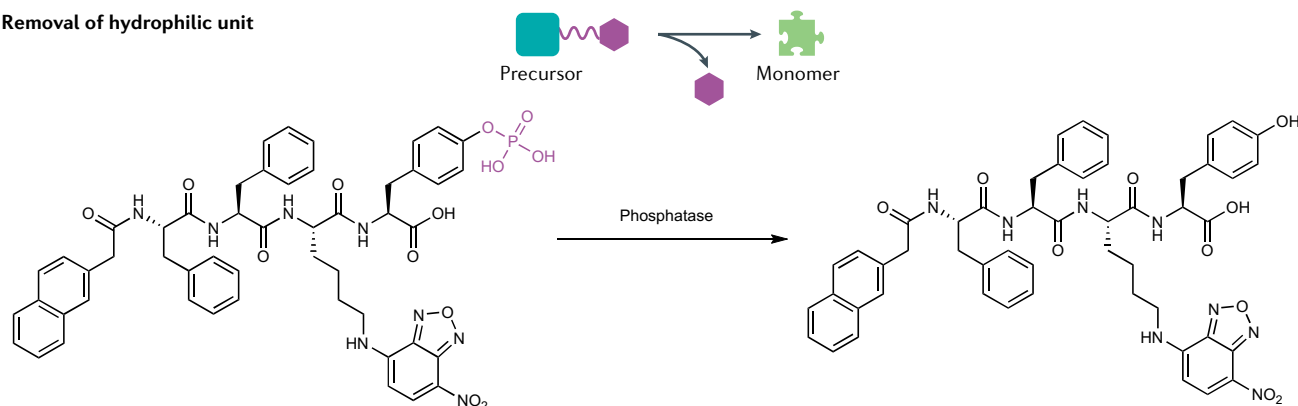
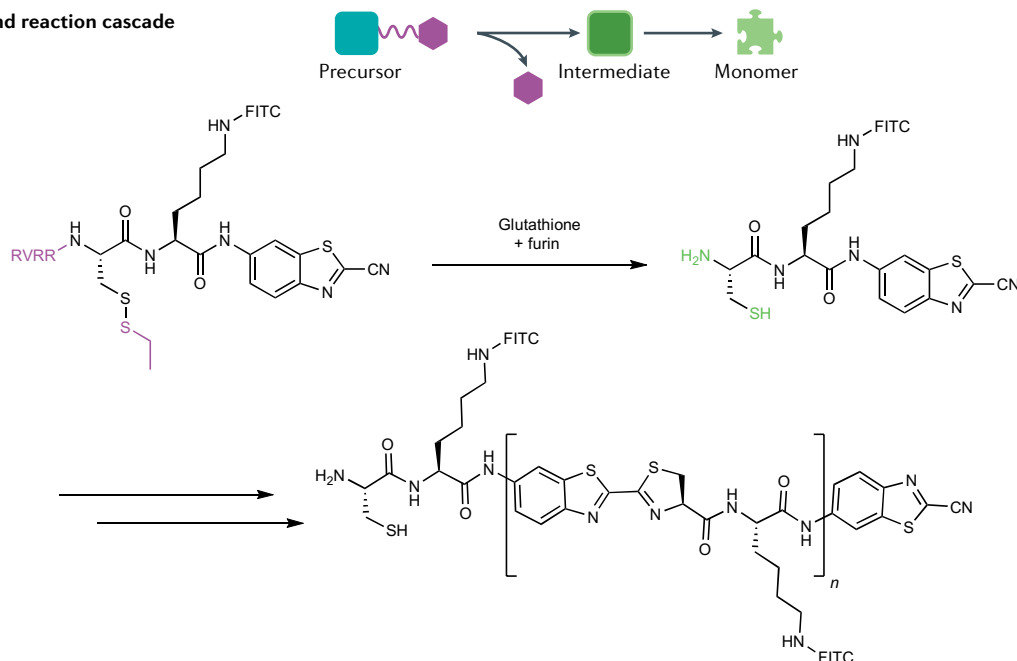
of a peptide sequence prone to hydrogen bonding and a nonpolar alkyl chain (fatty acid) engaging in hydrophobic interactions. Because of their fast assembly into dynamic but stable nanostructures and their gelation propensity<sup>64</sup>, these biocompatible amphiphilic conjugates have been studied extensively for various medical applications, including tissue regeneration<sup>65</sup> and wound healing<sup>66</sup>. Besides extracellular applications, their potential for intracellular structure formation and gelation has been used for enzyme-responsive and pH-responsive self-assembly inside cancer cells<sup>67,68</sup>.

Polyaromatic compounds can form intracellular aggregates because of  $\pi$ - $\pi$  aromatic interactions within the aqueous cytoplasm, which has been exploited for the creation of supramolecular imaging agents<sup>15</sup> and drugs for photodynamic therapy<sup>40</sup>. Prominent examples include bispyrene-based systems that rely on the formation of highly fluorescent *J*-aggregates<sup>69,70</sup> and luminogens that display aggregation-induced emission (AIE) properties<sup>71–74</sup>. Aside from fluorophores and AIE luminogens that display a constant number of aromatic rings both in the precursor and in the self-assembling monomer, there are also systems that rely on the intracellular formation of new aromatic units due to chemical transformation. For instance, the intracellular condensation reaction between a deprotected aminothioliol and an aromatic nitrile can be used to generate self-assembling aminoluciferin-based macrocycles inside cells<sup>9,75</sup>. This approach relies on the intracellular creation of polyaromatic cyclic oligomers that can self-assemble into fluorescent nanoaggregates via  $\pi$ - $\pi$  stacking<sup>9</sup>.

Stimuli-induced chemical transformations yielding a self-assembling monomer can be grouped by different



**Fig. 2 | Material classes for intracellular self-assembly.** Peptides represent the largest subset of nanomaterials for intracellular structure formation and can self-assemble into peptide nanofibres due to hydrogen bonding and  $\pi$ - $\pi$  stacking caused by aromatic amino acid residues<sup>59</sup>. In the case of peptide amphiphiles, hydrophobic interactions of alkyl chains also contribute to the self-assembly propensity<sup>67,68</sup>. Polyaromatic compounds form fibrous structures or nanoparticles because of aromatic interactions between the monomers<sup>9,69–74</sup>. Polymers, such as polyvinyl alcohol, transform into spherical aggregates or fibres<sup>14,58</sup>, whereas metal nanoparticles can aggregate into larger assemblies due to covalent crosslinking of their coating<sup>59–61</sup>.

**a Morphological transformation**

**b Removal of hydrophilic unit**

**c Deprotection and reaction cascade**


**Fig. 3 | Differences in complexity of the chemical transformation for intracellular self-assembly. a** | Morphology transformation due to *trans/cis*-amide isomerization<sup>84</sup>. **b** | Removal of a hydrophilic group in a phospho-tyrosine-containing peptide<sup>18</sup>. **c** | Deprotection of a bioresponsive cyclization precursor and following reaction cascade<sup>9</sup>. FITC, fluorescein isothiocyanate.

levels of complexity, depending on the length of the reaction sequence (FIG. 3). Generally, the molecular design concepts for bioresponsive self-assembly can be divided into three categories: structures that undergo a purely morphological transformation (FIG. 3a), pro-assembling monomers that transform into active monomers due to

the removal of a hydrophilic group (FIG. 3b) and molecules that rely on the bioresponsive deprotection of reactive groups causing a multistep reaction cascade (FIG. 3c). While the macrocyclization-based systems fit the last category, the most common strategy for controlled intracellular self-assembly uses the chemical or



enzymatic removal of a hydrophilic unit to trigger the aggregation of the remaining less polar fragment. By contrast, purely morphological transformations comprise systems that do not require the breakage of chemical bonds to transform into active monomers but instead rely on pH-induced isomerization or protonation.

Apart from materials that rely on bioresponsive transformations for self-assembly, local accumulation can also lead to aggregation, which does not depend on any specific endogenous stimulus<sup>76</sup>. A subcellular accumulation occurs by integrating organelle-specific targeting groups into the nanomaterial design, which can be exploited to locally exceed the critical aggregation concentration. For example, the positively charged targeting group triphenylphosphonium (TPP) has been used to induce the mitochondria-specific accumulation of short aromatic peptides, which leads to cellular dysfunction and cancer cell death<sup>77–79</sup>. Besides TPP, methylpyridinium-substituted materials also target the mitochondria: a methylpyridinium-containing oligothiophene conjugate revealed time-dependent and temperature-dependent accumulation and self-assembly first in the mitochondria, followed by the perinuclear region. The aggregation process was indicated by changes in fluorescence due to a bathochromic shift upon formation of superstructures<sup>80</sup>. For targeting the nucleus, lysine-rich peptides that bind to RNA can direct the self-assembling material to the desired organelle<sup>81</sup>.

### Physiological stimuli

Although a high local concentration of active monomers is the basis for assembly, the specificity and control over structure formation can be enhanced by leveraging physiological cues. The next sections are dedicated to the exploration of strategies for bioresponsive stimuli-induced self-assembly and the ways in which it allows for spatiotemporal control over the formation of intracellular nanostructures. Thus, the following sections are divided according to the respective chemical or biological stimulus that triggers the conversion of a pro-assembling precursor into an active monomer that can form supramolecular structures inside living cells.

### pH

The physiological pH in tissues and inside cellular organelles depends on a multitude of factors and represents an important parameter for biological processes. Moreover, compared with healthy tissue, the tumour microenvironment is often characterized by a slightly acidic pH (6.7–7.1), which is attributed to the enhanced glycolytic rate of cancer cells that results in hypoxia and acidification of the immediate extracellular matrix<sup>82</sup>. Inside cells, the endocytic pathway is accompanied by a pH gradient ranging from 6.3 in the early endosomes to 5.5 in the late endosomes and 4.7 in the lysosome<sup>83</sup>. In these cellular vesicles, a unique acidic environment is created, in which proteolysis and recycling of unneeded cellular components and waste take place.

These changes in pH during the entry of a certain cellular compartment can serve as an endogenous trigger for the self-assembly or the morphological

transformation of a pH-responsive nanomaterial<sup>8,10,11,84</sup>. Functional groups that are susceptible to protonation or deprotonation within physiological pH ranges can be found in the side chain residues of amino acids, making peptides a suitable platform for controlling pH-driven self-assembly. For example, a block co-polypeptide composed of a hydrophilic oligoarginine ( $R_{12}$ ) and an amphiphilic peptide with a repeating FKFE motif undergoes a morphological transformation upon endocytosis<sup>8</sup>. Inside the acidic late endosomes and lysosomes (pH  $\leq 5$ ), the protonation of glutamic acid residues (E) increases the hydrophobicity of the  $\beta$ -sheet-forming peptide and, therefore, its propensity for self-assembly. This causes a pH-driven morphology transition of the amphiphilic peptide — from unstable aggregates outside of the cell to defined vesicular structures inside the acidic compartments. As this supramolecular process correlates with a spatially confined increase in positive surface charge density of the nanostructures only within the acidic endosomal and lysosomal environments, the pH-responsive peptide exhibits a low cytotoxicity<sup>8</sup>. The high positive surface charge density of the locally formed vesicles is also responsible for the therapeutic effect of the nanomaterial as a supramolecular anti-proliferation drug because it suppresses the misfolding of proteins through electrostatic interactions.

While the acidification of extracellular pH and a slightly elevated cytosolic pH are seen as typical for metastatic cancer cells<sup>82</sup>, the core of solid tumours usually displays hypoxic cells with a slightly lowered intracellular pH caused by the accumulation of acidic metabolites such as lactate<sup>85</sup>. To exploit this particular phenomenon of pH dysregulation, a peptide amphiphile was designed that can self-assemble below pH 7 (REF.<sup>68</sup>) (FIG. 4a). The palmitoylated hexapeptide contains three carboxy-terminal glutamic acid residues that render the molecule sensitive to protonation-induced transformation at only slightly acidic pH levels, which is likely due to  $pK_a$  variations of the side chain carboxylic acids<sup>86</sup>. Consequently, the formation of cytotoxic fibres of the peptide amphiphile was observed exclusively inside cells with decreased intracellular pH, for example, HeLa cervical cancer cells (in vitro and in vivo) or HEK293 cells at the core of spheroids<sup>68</sup>.

Besides incorporating ionizable groups into the chemical design of a bioresponsive material, the use of structural elements prone to pH-dependent isomerization can also lead to the controlled formation of intracellular assemblies<sup>11,84</sup>. The relationship between bioactivity and pH-dependent morphology transformation is exemplified by a self-assembling pentapeptide with a central 4-amino proline capable of pH-sensitive *cis/trans*-amide isomerization in a physiological environment (FIG. 4b). Without the need for enzyme catalysis, which is a prerequisite for the isomerization of proline in native proteins<sup>87</sup>, the 4-amino-proline-based scaffold can switch from  $\beta$ -sheet-dominated helices at neutral pH to random-coil peptide nanoparticles at pH 6.5. Acidification inside the tumour microenvironment causes the dominance of the *trans*-isomer and, therefore, the formation of globular assemblies, whereas endocytosis and endosomal escape into the neutral cytosol

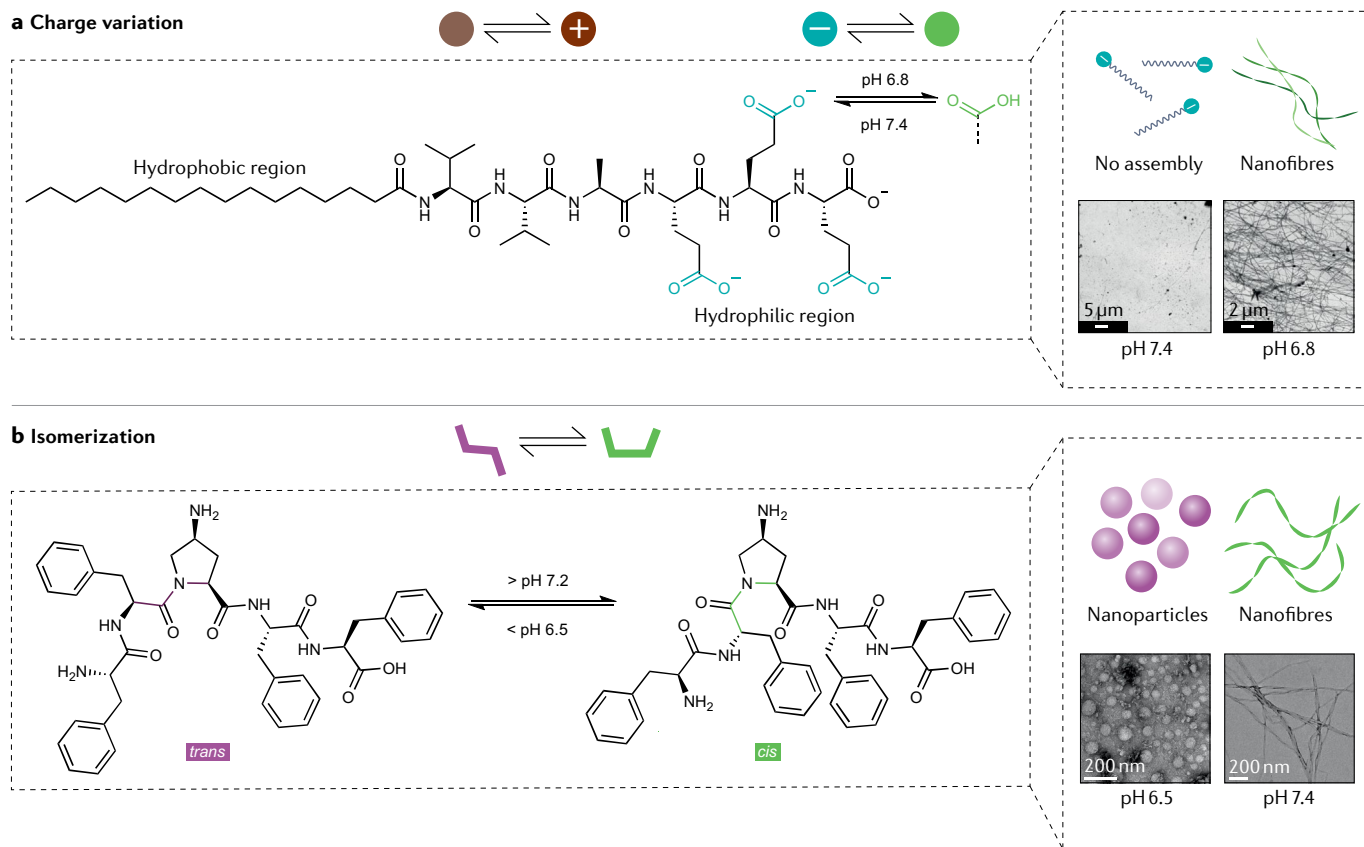


**Fig. 4 | pH as stimulus for intracellular self-assembly or morphology transformation.** **a** | Protonation of glutamate residues due to the acidification inside cancer cells with abnormally low cytosolic pH induces supramolecular assembly of a peptide amphiphile, as shown by the transmission electron microscopy images at pH 7.4 and 6.8 (REF.<sup>68</sup>). **b** | *trans/cis*-isomerization of pH-sensitive 4-amino proline causes the morphology transformation of a pentapeptide during cell entry. The transmission electron microscopy images show a transition from nanoparticles at pH 6.5 to nanofibres at pH 7.4 (REF.<sup>84</sup>). Part **a** (right) is adapted with permission from REF.<sup>68</sup>, American Chemical Society. Part **b** (right) is adapted with permission from REF.<sup>84</sup>, American Chemical Society.

triggers a *trans*–*cis* isomerization, resulting in a second morphology transformation to superhelical structures inside the cell<sup>11,84</sup>.

### Glutathione

Glutathione is the most abundant low-molecular-weight peptide in eukaryotic cells and consists of three amino acids: glutamate, cysteine and glycine<sup>37</sup>. Due to the reactive thiol group of its cysteinyl moiety, it acts as a reducing agent, a nucleophile and a cell-protective antioxidant, ensuring redox homeostasis by scavenging free radicals, such as ROS, lipid peroxides and heavy metals<sup>88</sup>. Normal levels of glutathione in human tissues range from 0.1 mM to 10 mM (REF.<sup>55</sup>), in which 85% to 90% of reduced glutathione is localized in the cytosolic–nuclear compartment<sup>89</sup>, transforming it into a reducing environment for both endogenous compounds and xenobiotics. Many cancers exhibit elevated levels of intracellular glutathione that correlate with higher cellular proliferation and metastatic activity<sup>90,91</sup>, as well as multidrug resistance caused by an increased efflux of glutathionylated chemotherapeutics<sup>92</sup>. Glutathione, therefore, constitutes an attractive endogenous stimulus for controlled intracellular self-assembly, due to its ubiquity

in cells, its capability of efficiently reducing disulfide bonds and the significant difference in its distribution inside and outside of the cell<sup>93</sup>.

The reduction and cleavage of a disulfide bond by glutathione can cause the removal of a hydrophilic aggregation-inhibitive unit, thereby, releasing the self-assembling component to form the designated nanostructures inside the cell<sup>12,15,58,94</sup>. An example for this strategy is the glutathione-responsive fluorescence probe that is composed of a bispyrene linked to a positively charged cyanine dye via a disulfide bridge<sup>15</sup>. Glutathione-induced cleavage of the disulfide in the cytosol causes the separation of the two fluorophores, thereby, allowing the free bispyrene to form large, highly fluorescent *J*-aggregates<sup>69</sup> in vitro and in vivo<sup>15</sup>. Aside from this small molecule probe for the imaging of glutathione levels, glutathione-responsive polymer–peptide conjugates have also been synthesized<sup>58</sup>. These conjugates consist of a thermoresponsive poly(*N*-isopropylacrylamide) backbone covalently linked to a hydrophilic cell-penetrating peptide by a disulfide bond (FIG. 5a). Upon glutathione-induced cleavage, the polymer conjugate exhibits a decrease in lower critical solution temperature to below 37 °C,

**Xenobiotics**  
Substances that are foreign to the organism.

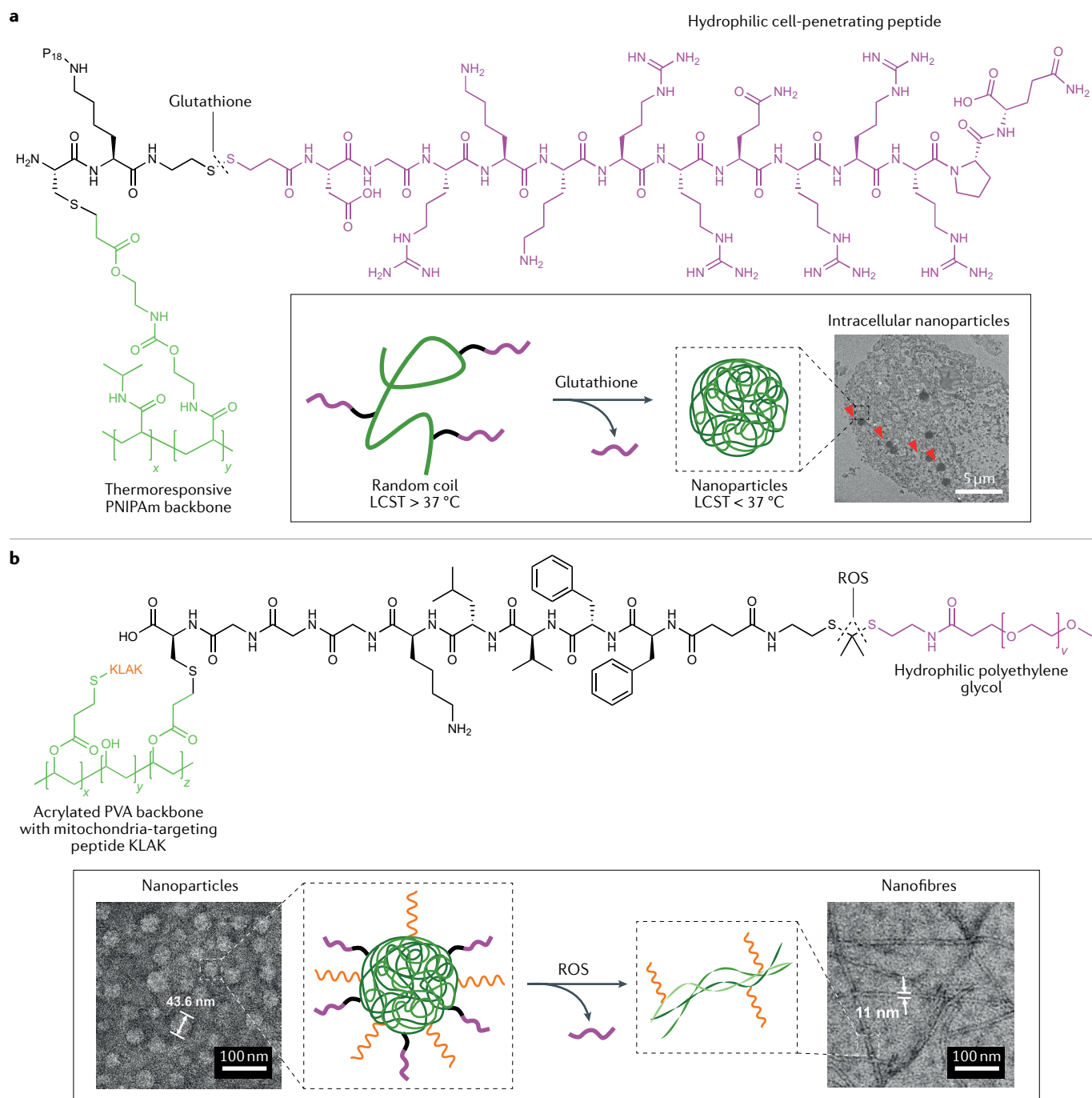


Fig. 5 | **Redox-induced intracellular self-assembly.** **a** | Glutathione-induced cleavage of a disulfide bond changes the lower critical solution temperature (LCST) behaviour of a polymer conjugate, causing it to form intracellular nanoaggregates<sup>58</sup>. Bio-transmission electron microscopy of MC7 cells shows the presence of intracellular nanoparticles. **b** | Cleavage of a reactive oxygen species (ROS)-sensitive thioketal group induces fibre formation<sup>14</sup>. Transmission electron microscopy images show ROS-induced transformation from nanoparticles to nanofibres in hydrogen-peroxide-containing phosphate buffer. KLAKE, mitochondria-targeting peptide; P<sub>18</sub>, purpurin 18; PNIPAm, poly(*N*-isopropylacrylamide); PVA, polyvinyl alcohol. Part **a** (right) is adapted with permission from REF.<sup>58</sup>, American Chemical Society. Part **b** (bottom left and right) is adapted with permission from REF.<sup>14</sup>, American Chemical Society.

which causes a transition from a random-coil state into spherical aggregates inside the cell. In addition, this system can be tuned to respond to different endogenous stimuli, including the proteolytic cleavage of the hydrophilic peptide by various enzymes, for example, caspase-3 (REF.<sup>58</sup>).

### Reactive oxygen species

ROS are generated during mitochondrial oxidative metabolism<sup>56</sup> and as a cellular response to xenobiotics, cytokines and bacterial invasion<sup>95,96</sup>. Controlled ROS production inside the cell fulfils many biological purposes, such as the regulation of signal transduction<sup>56,97</sup>



with regards to angiogenesis<sup>96</sup> and insulin metabolism<sup>98</sup>. However, overproduction of ROS leads to oxidative stress and is linked to various pathological phenomena<sup>99</sup>, including abnormal cell growth that can perpetuate cancer initiation and progression<sup>100,101</sup>.

Targeting cancer cells with high levels of ROS<sup>102</sup> for oxidation-driven self-assembly is a relatively new strategy to create supramolecular architectures inside cells<sup>6,14</sup>. The mitochondria produce ROS by means of the electron transport chain<sup>103</sup>, thereby, influencing the immediate redox environment of the organelle and making it an attractive subcellular target for ROS-sensitive materials. Thioketals are an example of a ROS-sensitive functionality that can be degraded in the presence of sufficient amounts of cellular oxidants<sup>104</sup>. For instance, using a thioketal linker to attach a hydrophilic polyethylene glycol (PEG) chain to a self-assembling peptide on a polymer backbone, that is also decorated with a mitochondria-targeting peptide (KLAK), gives rise to a multifunctional platform for mitochondria-specific accumulation, morphology transformation and assembly<sup>14</sup> (FIG. 5b). This polymer-peptide conjugate consisting of two different polymers (PEG side chain and polyvinyl alcohol backbone), as well as two different peptides (KLAK and  $\beta$ -sheet-forming peptide), can enter the cells as a nanoparticle and undergoes a transformation into a fibrous network in the proximity of ROS-overproducing mitochondria. The morphological transformation is designed in a way that a lipophilic  $\beta$ -sheet-forming sequence is flanked by two hydrophilic polymers, KLAK-functionalized polyvinyl alcohol and PEG. In this initial state, the chains collapse into spherical aggregates, where the steric component of two bulky hydrophilic polymers prevents molecular interaction between the  $\beta$ -sheet peptides. Upon oxidation by high amounts ( $\mu\text{M}$ ) of ROS, the PEG segment is cleaved, transforming the molecule into an amphiphilic structure. Hence, the steric hindrance is relieved and chain flexibility promotes intermolecular interactions between

interchain  $\beta$ -sheet peptides to afford a fibrillar morphology. The ROS-sensitive supramolecular system exhibits significantly higher cytotoxicity towards HeLa cervical cancer cells than towards normal cells, both in vitro and in vivo<sup>14</sup>.

### Enzymes

Biocatalytic reactions carried out by enzymes enrich the chemical depth of cellular pathways, allowing molecules and biopolymers to be processed within the environmental limitations of a living system. Besides converting natural substrates, many enzymes have also been exploited for the intracellular transformation of synthetic precursors into self-assembling monomers<sup>18,50,105,106</sup> (TABLE 1). For this purpose, enzyme-specific recognition motifs can be included in the molecular design of the precursor to tailor its bioresponsiveness towards a certain enzyme within the cell (FIG. 6). The following sections highlight the use of various types of intracellular enzymes, namely, proteases, phosphatases and other kinds of enzymes, to instruct targeted structure formation at different subcellular locations.

**Proteases.** Proteolytic enzymes catalyse the hydrolysis of peptide bonds<sup>107</sup>, making them an attractive biological tool for the activation of bioresponsive nanomaterials. The diversity of proteases in terms of their subcellular localization, level of expression in different cell types, as well as their specificity for a certain cleavage site, facilitates spatiotemporal programming of enzyme-instructed self-assembly.

Furin is an endoprotease that is associated with the Golgi apparatus in eukaryotic cells. Belonging to the enzyme family of propeptin convertases, it catalyses downstream peptide cleavage of the polybasic motif RX(R/K)R for the bioactivation of certain proteins<sup>108</sup>. This enzymatic cleavage reaction plays an essential role in pathogenesis, as the enzyme activity of furin has been linked to cancer progression<sup>109,110</sup>, as well as viral diseases<sup>111</sup>, including SARS-CoV-2 infection<sup>112</sup>. Therefore, the imaging of furin activity inside cells or tumour tissue is an attractive target that can be addressed using bioresponsive supramolecular chemistry. For example, the intracellular condensation reaction between an aminothiols and a cyanobenzothiazole for the formation of self-assembling macrocyclic dimers was first realized using a furin-sensitive precursor (FIG. 3c). By adding the four amino acids RVRP to the amino-terminal cysteine, they serve not only as an enzyme-cleavable protecting group (FIG. 7a) for the amino function but also facilitate cell entry of the precursor due to the positively charged side chain residues<sup>9</sup>. Further investigation of the intracellular reaction cascade showed that the furin-induced proteolytic cleavage near the Golgi apparatus constitutes the rate-limiting step for the formation of active monomers, which correlates to the subcellular localization of the resulting nanostructures at this site<sup>21</sup>. This enzyme-instructed intracellular aggregation also enables in vivo imaging of furin activity inside furin-overexpressing tumour tissue, since it can promote the accumulation and retention of an imaging agent that is covalently linked to the

Table 1 | Enzyme-instructed intracellular self-assembly

Enzyme	Transformation site	Cellular localization	Refs
Furin	RVRP_	Golgi	9,21,60,61,113–118,183
Caspase-3/7	DEVD_	Cytosol	16,22,39,48,50,58,59,123,125
ENTK	DYKDDDDK_	Mitochondria	106,133–135
ATG4B	TFG_F	Cytosol	58,157
Cathepsin B	GF_LG	Lysosome	5,40
ALP	Yp	Cell membrane	17,18,20,53,57,163,164,167,180,184–189
PTP1B	Yp	ER	17,18,163,164,166,186
$\beta$ -Galactosidase	$\beta$ -Gal-aromatic	Lysosome	16,171
$\gamma$ GT	$\gamma$ -E_	Cell membrane	190
Nitroreductase	$-\text{NO}_2 \rightarrow -\text{NH}_2$	Cytosol	178
Transglutaminase	$\rightarrow \epsilon-(\gamma\text{-Q})\text{-K}$	Cytosol, ER, mitochondria	105
Carboxylesterase	Ester bond	ER	51,173–176

$\gamma$ GT,  $\gamma$ -glutamyltransferase; ALP, alkaline phosphatase; ATG4B, autophagy-related 4B cysteine peptidase; ENTK, enterokinase; ER, endoplasmic reticulum; PTP1B, protein tyrosine phosphatase 1B.

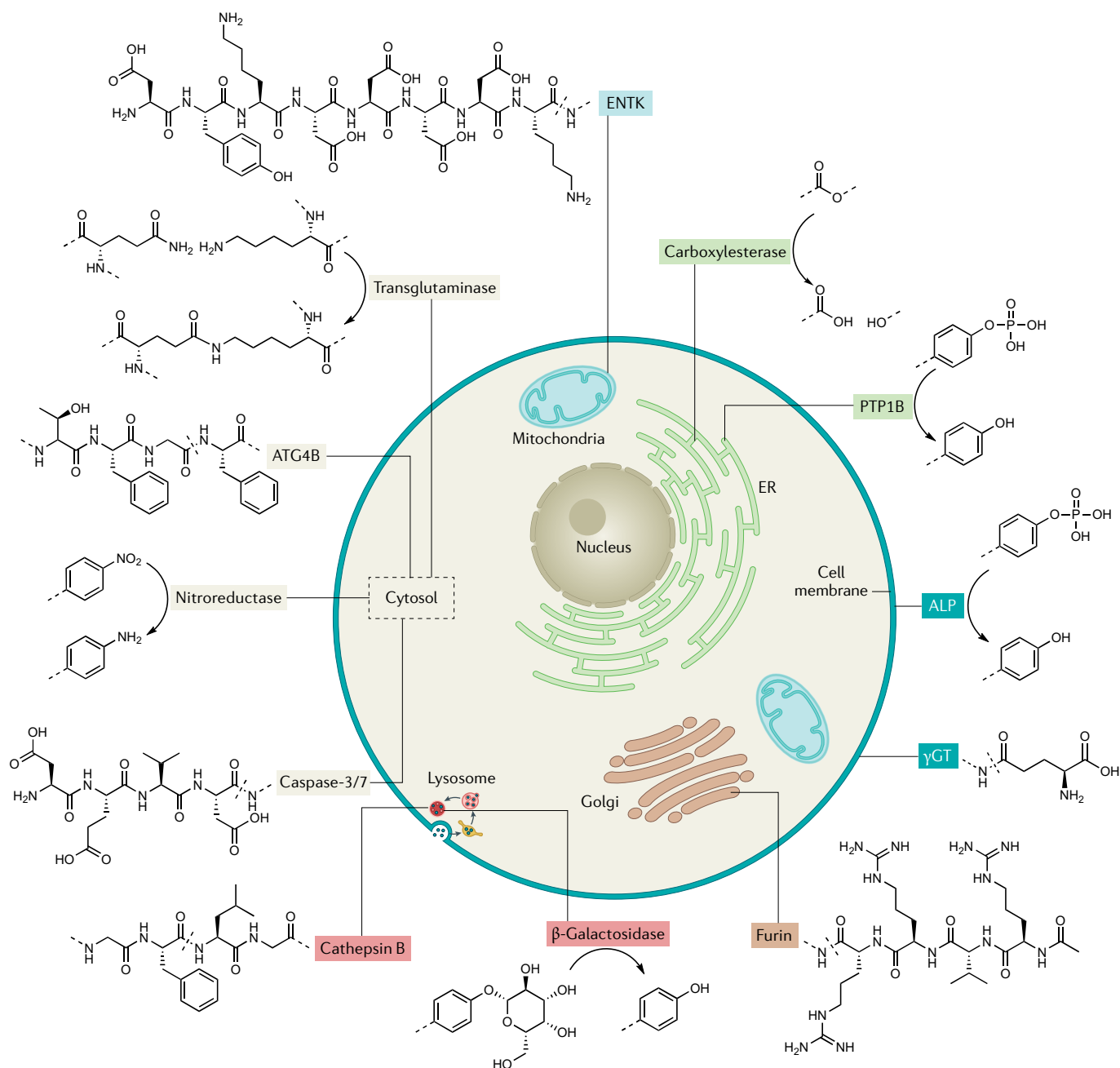
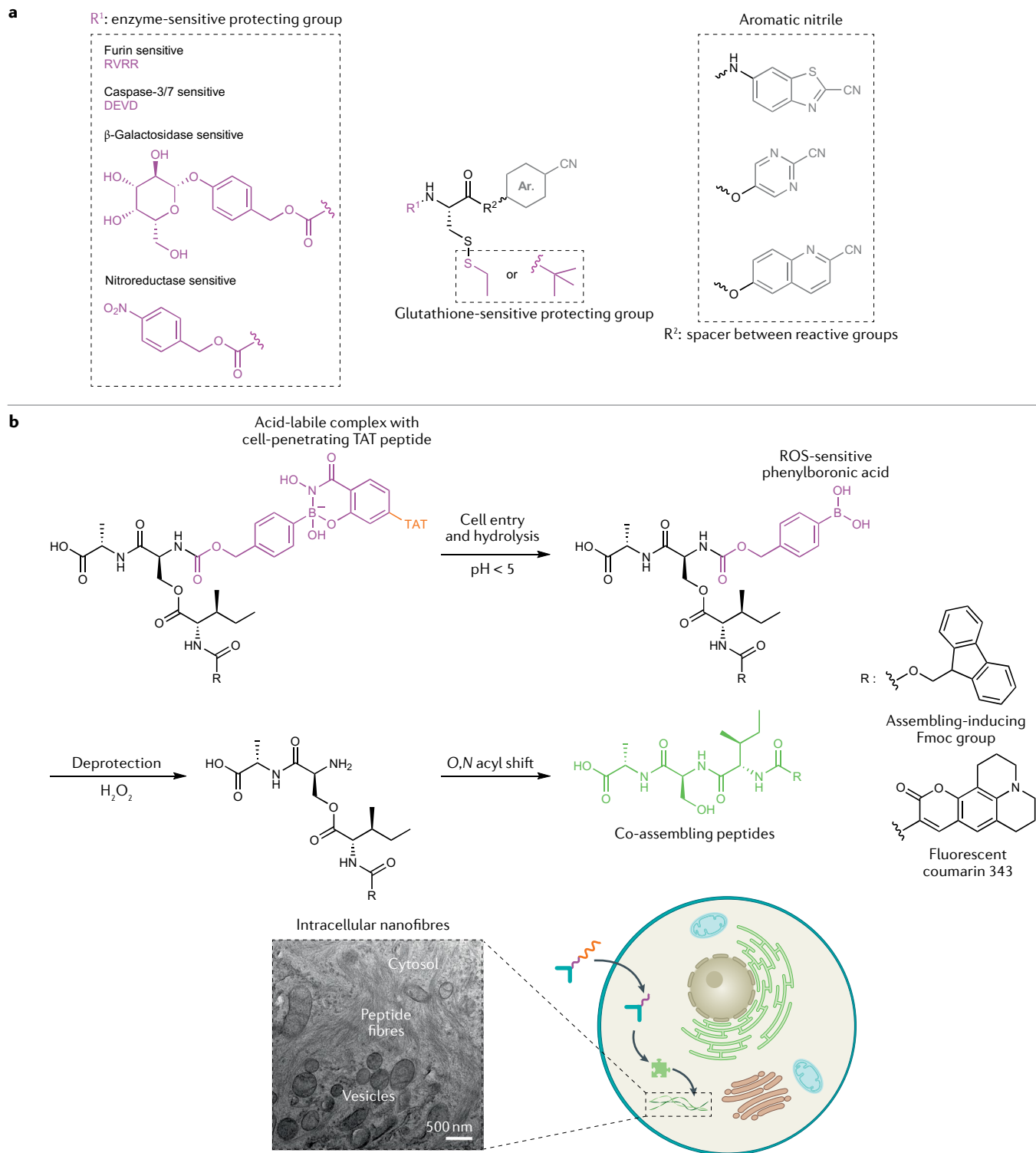


Fig. 6 | **Cellular localization of enzymes for self-assembly and their respective recognition and transformation sites.** γGT, γ-glutamyltransferase; ALP, alkaline phosphatase; ATG4B, autophagy-related 4B cysteine peptidase; ENTK, enterokinase; ER, endoplasmic reticulum; PTP1B, protein tyrosine phosphatase 1B.

self-assembling monomer. A variety of techniques that exploit this effect have been applied for diagnostic purposes, such as photoacoustic imaging<sup>113</sup>, micro-positron emission tomography<sup>114</sup>, use of radiotracers<sup>115</sup>, Raman imaging<sup>116</sup> and magnetic resonance imaging<sup>117</sup>. In all these studies, the imaging agent was introduced to the precursor molecule via side chain modification of a lysine positioned between the cyanobenzothiazole and the cysteine. The use of this strategy for the chemical modification of the condensation precursor has also been used for the conjugation of the chemotherapeutic drug, Taxol, which helps to prevent undesired drug

efflux and promotes sustained drug release due to the furin-induced self-assembly of Taxol nanoparticles<sup>118</sup>. Aside from the attachment of small organic molecules, metal-based nanoparticles can also be decorated with the bioresponsive precursor by using the amino group of the lysine side chain for amide coupling reactions on a carboxyl-modified particle surface<sup>60,61</sup>. The resulting metal-based pro-assembling nanomaterials can form aggregates of gold or iron oxide nanoparticles inside furin-overexpressing cells as a result of particle crosslinking caused by enzyme-triggered condensation reactions.



**Fig. 7 | Multistep transformation for intracellular self-assembly.**  
**a** | Structures of assembly precursors for macrocyclization-based self-assembly. The amino protecting group determines the sensitivity to a specific enzyme, such as furin<sup>9,21,113</sup>, caspase-3/7 (REFS<sup>16,50,125</sup>),  $\beta$ -galactosidase<sup>16</sup> or nitroreductase<sup>178</sup>. The peptide-based spacer  $R^2$  between the reactive functionalities can contain fluorophores, drugs or other bioactive compounds. **b** | Multistep reaction sequence of intracellular conversion pH-sensitive and reactive oxygen species (ROS)-sensitive isopeptides into linear co-assembling peptides. The targeting group contains cell-penetrating peptide TAT (transactivator of transcription) and

enables cell entry, upon which the acid-labile dynamic covalent bond between the salicyl hydroxamate of targeting peptide and the phenylboronic acid group of the isopeptides is hydrolysed in the endosomes. The hydrogen-peroxide-induced deprotection via self-immolation of the phenylboronic acid group reveals a reactive amino group that can attack the adjacent ester bond. This rearrangement due to an O,N acyl shift results in the linearized co-assembling peptides. The formation of peptide nanofibres inside A549 cells can be visualized with bio-transmission electron microscopy. Part **b** (bottom left) is adapted with permission from REF.<sup>6</sup>, American Chemical Society.

## Theranostic

Combining therapeutic and diagnostic properties within a single material platform.

Caspases are proteolytic enzymes that play an essential role in the initiation and execution of apoptosis, a mode of programmed cell death<sup>119</sup>. These endoproteases contain a characteristic nucleophilic cysteine as a central part of a polybasic substrate-binding pocket<sup>120</sup>. The chemical structure of their active site enables them to catalyse the hydrolytic cleavage of proteins for the controlled dismantling of the cell. Within the intricate activation cascade of different caspases, the so-called 'effector' caspases-3, 6 and 7 carry out most of the proteolysis during apoptosis and can, therefore, be considered biomarkers for programmed cell death<sup>121</sup>. Since caspase-3 and caspase-7 both exhibit similar preferential downstream cleavage of the motif DEVD in synthetic substrates<sup>122</sup>, many supramolecular systems have been designed to include this sequence as a bioresponsive moiety for intracellular self-assembly<sup>16,22,39,48,50,58,59,123–125</sup> (FIG. 6). For example, a fluorescent probe for the real-time imaging of apoptosis in drug-treated cancer cells was combined with the hydrophobic tetraphenylethene (TPE) with the hydrophilic peptide motif DEVD\_K via azide-alkyne click chemistry<sup>123</sup>. After enzymatic cleavage by caspase-3/7, the polyaromatic fragment TPE-K can self-assemble inside cells, which results in AIE caused by the restriction of intramolecular rotation of its phenyl rings<sup>126</sup>. These so-called AIE luminogens<sup>127</sup> — which exhibit a turn-on fluorescence upon aggregation — can be useful reporters of enzyme activity in cancer cells, especially when they are part of a multifunctional theranostic nanomaterial<sup>39</sup>.

A sequential approach to the caspase-induced formation of intracellular nanostructures uses systems containing tumour-specific recognition motifs able to trigger apoptosis<sup>22,48</sup>. A peptide-based precursor, containing a biomimetic sequence that can bind and inactivate the X-linked inhibitor of apoptosis protein (XIAP)<sup>128</sup>, promotes the activation of caspase-3/7 through the manipulation of intracellular signal transduction<sup>129</sup>. The activated pro-apoptotic proteases can then remove the non-assembling XIAP-recognition motif, thereby, inducing the self-assembly of the remaining  $\beta$ -sheet-forming peptide–drug conjugate<sup>48</sup> or peptide–cyanine dye conjugate<sup>22</sup>. This sophisticated system selectively causes assembly formation in cancerous tissue both in animal models and in ex vivo human bladders that were taken from patients with late-stage bladder cancer<sup>48</sup>. The latter experiment shows the potential clinical use of the caspase-sensitive assembly precursor, as it could help detect tumour boundaries during image-guided surgery.

For quantitative imaging of caspase-3/7 activity in live animals, a condensation-driven system was developed, in which the enzymatic activation of the precursor is decoupled from a subsequent imaging tag immobilization<sup>50</sup>. The pro-assembling molecule consists of the amino-terminal protecting group DEVD (FIG. 7a) linked to a cysteine, a lysine with a clickable *trans*-cyclooctene (TCO) on its side chain, as well as a pyrimidinocarbonitrile as the aromatic nitrile for the enzyme-instructed macrocyclization. Since this caspase-3/7-responsive molecule can form stable intracellular nanoaggregates, subsequent addition or

injection of a tetrazine-functionalized fluorophore leads to an immobilization of the imaging probe due to inverse electron demand Diels–Alder reactions between the tetrazine and the aggregated TCO-bearing monomers.

Enterokinase (ENTK) (also known as enteropeptidase)<sup>130</sup> is a membrane-bound protease that is essential for digestion<sup>131</sup>. Its main physiological purpose is the cleavage of the acidic motif DDDDK in the pancreatic proenzyme trypsinogen, which leads to the activation of trypsin<sup>132</sup>. There are multiple reasons as to why ENTK is an interesting enzyme candidate for programming cell-specific and organelle-specific self-assembly<sup>106,133–135</sup>: firstly, its role in the activation of trypsin has been linked to matrix degradation and migration of lung, colorectal and glioblastoma cancer cells<sup>136</sup>; secondly, it allows cell-specific targeting of the mitochondria in cancer cell lines, such as HeLa (cervical cancer), Saos-2 (bone cancer) and HepG2 (liver cancer)<sup>134</sup>; and, thirdly, it enables the enzyme-driven release of cargo from a supramolecular vehicle at the organelle surface<sup>133</sup>. The ENTK-sensitive systems consist of the cleavable FLAG-tag DYKDDDDK covalently linked to a self-assembling peptide sequence<sup>106,133,134</sup> or a lipid-like moiety<sup>135</sup>. The chemical design of the peptide-based precursor is a branched structure that is important for mitochondria targeting<sup>133</sup>. After entering the cell in a micellar form by clathrin-mediated endocytosis<sup>134</sup>, the supramolecular precursors escape the endosome facilitated by pH buffering of the carboxylic acid groups<sup>135</sup>. The subsequent subcellular accumulation at the mitochondria is promoted by the increased mitochondrial membrane potential in cancer cells and the electrostatic interaction between the negatively charged FLAG-tag and voltage-dependent anion channels at the organelle surface<sup>135</sup>. The enzymatic cleavage of the hydrophilic tag by ENTK initiates the local conversion from micelles to peptide nanofibres<sup>106,133,134</sup> (or more lipophilic micelles in the case of the peptide–lipid conjugates)<sup>135</sup>. This supramolecular transformation causes an increase in perimitochondrial viscosity and enables the organelle-specific delivery of drugs<sup>133,135</sup>, proteins<sup>106</sup> or gene vectors<sup>134</sup>.

Trypsin is a potent serine protease that has been the subject of ongoing biomedical research due to its role in the invasion and metastasis of various cancers, such as ovarian<sup>137</sup>, colorectal<sup>138,139</sup>, lung<sup>140</sup> and prostate cancer<sup>141</sup>. The overexpression of different trypsin isoforms by tumours leads to the amplified degradation of extracellular proteins<sup>142</sup> and the increased activation of other matrix-associated proteases<sup>137,143,144</sup>. The preferential cleavage of trypsin at the carboxy terminal of lysine or arginine can be exploited as an enzymatic trigger for the self-assembly of synthetic monomers, as shown by a trypsin-responsive precursor molecule<sup>19</sup>. Similar to the ENTK-responsive systems, the branched pro-assembling peptide consists of an aromatic tetrapeptide backbone and a hydrophilic lysine-rich sequence KYDKKKKDG that can be cleaved in trypsin 1-overexpressing ovarian cancer cells (OVSAHO). As these particular cells exhibit an abnormally high activity of the protease at the endoplasmic reticulum (ER), the resulting formation

of cytotoxic nanofibres is not only cell specific but also organelle specific, despite high concentrations of the supramolecular precursor being necessary.

Cathepsin B is a lysosomal protease that has been linked to the invasiveness of several types of cancer<sup>145</sup>, including colorectal<sup>146</sup> and breast cancer<sup>147</sup>. This pro-angiogenic enzyme<sup>148</sup> recognizes and cleaves the sequence GFLG in synthetic substrates, which has made it a useful biological tool for cancer-specific drug delivery<sup>149</sup>. Combining the technology of AIE luminogens with a cathepsin B-cleavable peptide led to a light-up imaging probe and photosensitizer for the detection and ablation of breast cancer cells<sup>40</sup>. The precursor consists of a tetraphenylethylene derivative with two azido groups that are each 'clicked' to a bioactive peptide composed of the cathepsin B-responsive sequence GFLG, a hydrophilic linker (DDD) and the targeting moiety cyclo-RGD. The double-substituted AIE imaging probe can form fluorescent aggregates in the lysosomes of breast cancer cells (MDA-MB 231), which facilitates the quantification of enzyme activity, as well as photodynamic therapy<sup>40</sup>. To study the autocatalytic growth of intracellular nanofibres, a cathepsin B-responsive prodrug was developed that could undergo a morphology transformation from nanoparticles to fibrous networks *in vitro* and *in vivo*: after shedding a hydrophilic PEG-RGD unit, the remaining self-assembling peptide–drug conjugate undergoes  $\beta$ -sheet-driven fibrillation inside HeLa cells, which is accelerated by the presence of previously formed fibrils<sup>5</sup>.

Matrix metalloproteinase 7 (MMP7) is a protease involved in the degradation of extracellular matrix proteins<sup>150</sup>, contributing to cancer cell migration<sup>151</sup>. To initiate cancer cell death by intracellular self-assembly, a peptide–lipid conjugate susceptible to cleavage by MMP7 was developed, an enzyme that is secreted by HeLa cells<sup>67</sup>. The palmitoylated peptide consists of a glycine-rich nonpolar sequence, an MMP7 cleavage site (PLG\_L) and a hydrophilic carboxy-terminal fragment (\_LARK) that inhibits unspecific aggregation before enzymatic conversion. After incubation with the precursor, HeLa cells exhibited decreased viability caused by the cancer-cell-specific formation of intracellular peptide–lipid nanofibres<sup>67</sup>.

ATG4B is a cysteine protease that contributes to autophagy, during which protein aggregates and damaged organelles are digested and recycled<sup>152</sup>. While it is essential for homeostasis in healthy tissue, dysregulated autophagy is associated with pathogenesis, such as tumorigenesis<sup>153,154</sup> and neurodegeneration<sup>155</sup>. Since ATG4B is crucial for the formation of autophagosomes<sup>156</sup>, its activity was monitored using a bioresponsive supramolecular probe<sup>157</sup>. The chemical design of this imaging agent combines a self-assembling bispyrene with a peptide displaying the ATG4B cleavage site TFG\_F<sup>157</sup>, as well as a highly cationic poly(amidoamine) dendrimer that enables cell entry and provides water solubility. After the enzymatic cleavage in MCF-7 breast cancer cells, the free bispyrene units self-assemble into fluorescent nanoparticles due to the formation of *J*-aggregates<sup>69</sup>, before transforming into cytosolic nanofibres over time<sup>157</sup>.

### Phosphatases

Phosphorylation and dephosphorylation of protein substrates play a vital role in signal transduction and the regulation of enzyme and receptor activity<sup>158</sup>. Since dysregulation of these processes is associated with cellular dysfunction and tumorigenesis, phosphatases, which are the enzyme family responsible for the removal of phosphate groups<sup>159</sup>, are interesting candidates for controlling enzyme-instructed intracellular self-assembly. Alkaline phosphatase (ALP) is a prominent example of a ubiquitous enzyme that catalyses dephosphorylation<sup>160</sup>. Regarding subcellular localization, ALP as a membrane-bound phosphatase is associated with the cell membrane<sup>160</sup>, while PTP1B, another important protein tyrosine phosphatase, is located at the surface of the ER<sup>161</sup>. By exploiting the overexpression of both ALP and PTP1B as known tumour markers, phosphatase-instructed self-assembly of short phospho-tyrosine (Yp)-containing peptides can be used for bioimaging<sup>18</sup> and combinational cancer therapy<sup>162</sup>.

A general structure of the precursor for phosphatase-instructed self-assembly was established: a tetrapeptide containing two phenylalanines, one Yp that can be dephosphorylated, as well as a basic amino acid, such as lysine, which can be coupled to a fluorophore or a targeting unit. The amino terminus of the short peptide is substituted with an additional aromatic moiety, for example, a naphthyl group, that contributes to the propensity for self-assembly due to intermolecular aromatic interactions of the dephosphorylated monomer. For example, the fluorescent aromatic tetrapeptide naphthyl-FFK(nitrobenzoxadiazole (NBD)) Yp was used as a phosphatase-sensitive precursor for the formation of fluorescent nanofibres inside HeLa cells<sup>18</sup> (FIG. 3b). Interestingly, the fibrous structures were observed to grow within minutes from the ER towards the cell membrane, which can be explained by the high enzymatic activity of PTP1B at the surface of the organelle<sup>18</sup>. Besides using NBD as the dye, introducing other fluorophores revealed that the supramolecular behaviour and the spatial distribution of the intracellular assemblies vary drastically depending on the fluorescent unit<sup>163,164</sup>; NBD-containing monomers can form intracellular nanofibres that protect the cell and its cytoskeleton against an F-actin toxin, whereas dansyl-substituted peptide localizes in the cell membrane and exhibits a cytotoxic effect after dephosphorylation<sup>124</sup>. These differences in the bioactivity of the precursors and the respective activated monomers can be explained by variations in hydrophobicity of the fluorophore dictating both their interactions with cellular membranes and their self-assembly propensity. For example, the dansyl group exhibits a higher solubility in phospholipid membranes, partly due to its compatibility with the headgroup of phosphatidylcholine<sup>165</sup>, while the peptide precursor substituted with positively charged rhodamine cannot produce a hydrogel even after dephosphorylation by ALP, leading to an unspecific fluorescence distribution inside and outside of the cells<sup>124</sup>.

Aside from modulating the intracellular assembly behaviour by changing the fluorophore, exchanging amino acids with different stereochemical properties in

#### Autophagy

Ordered degradation and recycling of dysfunctional cellular components, which is important for homeostasis.

#### Tumorigenesis

Formation or emergence of cancerous cells.



the precursor can also change the morphology of the nanostructures resulting from dephosphorylation<sup>17</sup>. By attaching an L-homoarginine (<sup>4</sup>hR) at the carboxyl terminus of the D-tripeptides, naphthyl-<sup>D</sup>F<sup>D</sup>F<sup>D</sup>Yp and NBD-<sup>D</sup>F<sup>D</sup>F<sup>D</sup>Yp precursors were generated for phosphatase-instructed self-assembly that, after dephosphorylation, could form cytotoxic crescent-shaped assemblies targeted for accumulation at the ER. The toxic effect of the crescent-shaped structures seemed to be cell specific, as it was limited to cancerous cells with high levels of ALP at their cell membrane, such as HeLa cervical cancer cells and OVSAHO ovarian cancer cells, while normal stromal cells (HS-5) were not affected<sup>17</sup>.

To further control and exploit the subcellular localization of phosphatase-instructed assemblies, the structure of the precursor can be adapted for organelle-specific targeting<sup>57,166,167</sup>. Integrating positively charged TPP via lysine side chain modification gives rise to mitochondria-targeted tetrapeptides that can undergo dephosphorylation by ALP at the cell membrane of Saos-2 osteosarcoma cells<sup>57</sup>. The resulting polymorphic aggregates can enter the cells and trigger the release of cytochrome *c* from the mitochondria, causing cell death only in ALP-overexpressing cancer cells. The in situ generation of the self-assembling monomers seems to be essential for the toxicity towards the cells, since incubating them directly with the final product of the enzymatic conversion has no effect on their viability<sup>57</sup>. Aside from the use of well-known targeting moieties such as TPP, incorporating ligands of enzymes that are specific for a certain organelle can also influence the accumulation and structure formation at the desired subcellular location. An example for this is the naproxen (Npx)-substituted tetrapeptide Npx-<sup>D</sup>F<sup>D</sup>F<sup>D</sup>Yp<sup>4</sup>hR used for intracellular enzyme sequestration on the surface of the ER<sup>166</sup>. Npx is a nonsteroidal anti-inflammatory drug and a ligand of COX2, which is an enzyme located at the surface of the ER. By binding to COX2 via Npx and to PTP1B via Yp, the precursor and the resulting fibrous assemblies can sequester the two enzymes on the organelle surface, thereby, inducing their co-localization and potential protein–protein interaction. Another recent discovery regarding organelle-specific phosphatase-instructed self-assembly was that short thiophosphopeptides can form nanofibres specifically at the Golgi apparatus<sup>167</sup>. This phenomenon seems to be due to the rapid conversion of thiophosphopeptides into thiopeptides by Golgi-associated ALP followed by disulfide bond formation with cysteine-rich proteins in the oxidative environment of the organelle.

**Other enzymes.**  $\beta$ -Galactosidase is a lysosomal sugar hydrolase that is overexpressed in senescent cells<sup>168</sup>. As the accumulation of non-proliferating cells can negatively impact tissue function<sup>169</sup>, detecting and clearing senescent cells is of therapeutic interest, especially for age-related diseases such as atherosclerosis<sup>170</sup>. For this reason, a short aromatic peptide was designed with a  $\beta$ -galactose-functionalized tyrosine (NBD-FFY( $\beta$ -Gal)G) that is susceptible to enzymatic cleavage inside senescent endothelial cells and HeLa cells<sup>171</sup>. While the viability

of non-senescent cells was only slightly affected by the administration of the enzyme-responsive precursor, it caused the  $\beta$ -galactosidase-instructed formation of cytotoxic nanofibres in senescent cells due to intermolecular aromatic interaction. A different approach to implement  $\beta$ -galactosidase sensitivity into a precursor for condensation-driven self-assembly used a benzyl carbamate amino protecting group with a  $\beta$ -galactose substituent on the aromatic ring that could undergo self-immolative degradation upon enzymatic removal of the sugar<sup>16</sup> (FIG. 7a). This  $\beta$ -galactosidase-induced deprotection of a reactive amino thiol triggers a subsequent condensation reaction with an aromatic nitrile that results in the intracellular formation of self-assembling macrocycles.

Carboxylesterases (CES) are essential for the cleavage of endogenous and xenobiotic esters<sup>172</sup>. Aside from their general importance for lipid homeostasis and drug metabolism, CES were also the first enzymes to be exploited for the intracellular self-assembly of synthetic nanomaterials<sup>173</sup>. The CES-responsive precursors generally consist of a diphenylalanine, an amino-terminal naphthyl group or aromatic fluorophore, and a carboxy-terminal ethanolamine offering a hydroxyl group for the esterification of a hydrophilic unit (for example, butyric acid or taurine) that prevents aggregation<sup>51,173–176</sup>. Inside cells with high CES activity, such as certain ovarian and cervical cancer cells, the enzymatic cleavage of the ester bond leads to the formation of nanofibres that can disrupt actin filaments<sup>175</sup> and boost the activity of the anticancer drug cisplatin<sup>51</sup>.

While the enzymes mentioned so far in this Review are all hydrolases, meaning that they catalyse the breakage of chemical bonds using water, there are also enzymes that create new bonds and that can be used for the programming of nanomaterial aggregation inside cells.

Transglutaminase is an enzyme that catalyses the amide bond formation between glutamine and lysine side chains<sup>177</sup>. This biocatalytic condensation reaction can be exploited for the intracellular polymerization of short peptide monomers into elastin-like polypeptides (ELPs)<sup>105</sup>. The topology and the thermoresponsive properties of these ELPs is predetermined by the number of lysines and glutamines in the polymerizable monomer: while peptide monomers with only one lysine and glutamine each yield linear ELPs with upper or lower critical solution temperature behaviour to form globular aggregates, monomers containing more than one lysine and glutamine yield a three-dimensional gel-like ELP network inside the cell. The latter exhibits a dose-dependent cytotoxicity, whereas linear ELPs forming random coils or aggregates are biocompatible<sup>105</sup>.

### Multistep conversion for self-assembly

The most common chemical design strategy for bio-responsive molecules for supramolecular assembly focuses on the combination of a cleavable hydrophilic unit with a more hydrophobic self-assembling moiety, such as a  $\beta$ -sheet-forming peptide or a polyaromatic group. In this general approach, the stimulus-induced separation of the two building blocks directly triggers

#### Senescent

Characteristic of cells with arrested cell cycle that can no longer divide but are still metabolically active. Cellular senescence is associated with multiple diseases later in life, such as cancer or atherosclerosis.

the formation of synthetic structures inside cells (FIG. 3b). However, given the complexity of the cellular environment and the many potential endogenous stimuli, systems for intracellular self-assembly can also be made to undergo a more complex multistep transformation to the final monomer. The idea of having a reaction sequence or cascade rather than a single transformative step also offers the opportunity to implement more than one bioresponsive element into the chemical design of the precursor, which can increase spatial control over the assembly formation.

The latter can be achieved, for example, by combining an enzyme-responsive unit on one part of the molecule with a redox-sensitive group on another part of the molecule (FIG. 7a). This combination has been used for the condensation reaction between a deprotected amino-thiol and a cyanobenzothiazole for the formation of self-assembling macrocycles<sup>75</sup>. As both the amino group and the thiol group of the amino-terminal aminothiol are necessary for condensation and self-assembly, choosing complementary bioresponsive protecting groups helps to tailor the system towards a specific intracellular behaviour. For example, the amino group of the aminothiol can be attached to an enzyme-responsive peptide sequence that is cleavable by a protease (for example, furin<sup>9,21,113</sup> or caspase-3/7 (REFS<sup>16,50,125</sup>)), while the thiol group can be protected via a disulfide bond to a small molecule such as ethanethiol (FIG. 7a). Upon cell entry, this disulfide bond is cleaved by intracellular glutathione in the reducing environment of the cytosol. Consequently, the determining step for the formation of the reactive intermediate, which can transform into the self-assembling monomer, is the final deprotection of the *N*-terminal amino group. As this can only occur at the subcellular localization of the targeted enzyme, spatial control over the structure formation is achieved by careful selection of the enzyme-responsive moiety in the precursor. This strategy is not only applicable to proteases but also works for other enzymes such as  $\beta$ -galactosidase<sup>16</sup> or nitroreductase<sup>178</sup> if a self-immolative benzyl-carbamate-derived protecting group is chosen for the amino terminus (FIG. 7a). The cyanobenzothiazole moiety can also be substituted for other less electrophilic aromatic nitriles, which lowers the risk of potential side reactions with endogenous aminothiols<sup>16</sup>. Aside from implementing bioresponsive groups that control self-assembly, additional enzyme cleavage sites can be included in the centre of the molecule that allow the programmed disassembly of intracellularly formed nanostructures by proteolysis later on<sup>16,17</sup>. For biomedical purposes, the cyclization precursor can be modified to include photothermal agents that are activated by condensation-mediated and assembly-mediated quenching<sup>13</sup> or chemotherapeutic drugs that can slowly be released inside tumour cells<sup>118</sup>.

For programming peptide fibre formation inside cancer cells, a multiresponsive system was designed that is pH sensitive and ROS sensitive<sup>6</sup>. The peptide-based precursors contain a phenylboronic acid trigger group, which serves as both a ROS-sensitive cage for the amino group of an esterified serine and as a handle for the attachment of a cell-penetrating peptide via an

acid-labile dynamic covalent bond (FIG. 7b). In the acidic environment of the endosome, the cell-penetrating peptide is removed. After endosomal escape, cytosolic ROS causes the degradation of the self-immolative phenylboronic acid group, revealing a free reactive amine. In the neutral pH of the cytosol, the nucleophilic amino group can perform an intramolecular attack on the adjacent ester bond of the serine side chain, yielding linearized peptides that can co-assemble into cytotoxic peptide fibres inside ROS-overproducing cancer cells<sup>5</sup>. These decoupled steps of the reaction cascade — the initial activation by deprotection and the following transformation to the monomer — take place under different chemical conditions and display individual reaction kinetics. Therefore, the multistep approach offers more opportunities to modulate the speed of the transformation of a precursor into a self-assembling monomer, in contrast to most systems for intracellular self-assembly that rely on a singular transformative step.

### Conclusions and outlook

Synthetic supramolecular chemistry in a cellular environment uses a strategic implementation of bioresponsiveness in chemical design to achieve control over the formation of nanoscale architectures. In this Review, we discuss various chemical scaffolds, such as peptides, polyaromatic molecules and polymers, that can undergo a triggered transformation into assemblies due to endogenous stimuli. Tailoring the reactivity of the nanomaterial towards a specific intracellular cue can be realized by incorporating redox-sensitive or pH-sensitive groups, as well as enzyme recognition motifs that allow biocatalytic transformations. These stimulus-dependent mechanisms of self-assembly come with numerous advantages for therapeutic or diagnostic application. For example, the bioresponsive properties of the materials contribute to cell and tissue specificity *in vivo*, while also allowing for spatial control over the structure formation inside cells by targeting organelle-specific enzymes. Another therapeutic advantage of systems for intracellular self-assembly is the circumvention of multidrug resistance in certain cancers due to an impaired efflux of the intracellularly formed nanostructures compared with small molecules. Moreover, this accumulation effect can also contribute to the concentration of fluorescent agents inside the targeted cells, enabling more efficient bioimaging. Compared with *ex situ* self-assembled materials, such as therapeutic nanoparticles, the monomeric assembly precursors generally display an easier clearance from the liver, spleen or kidneys, thereby, reducing their systemic toxicity<sup>179</sup>.

However, there are also several challenges regarding the potential clinical translation that need to be addressed. For example, a detailed pharmacokinetic and pharmacodynamic analysis of nanomaterials for intracellular self-assembly is necessary to ensure a favourable biodistribution and circulation time of precursors, as well as low immunogenicity. The chemical stability of the precursor molecule is crucial for its *in vivo* application, as, for instance, the proteolysis of peptide-based materials prior to cell entry and self-assembly needs to be avoided. Additionally, the eventual clearance of

the in situ-formed nanostructures must be considered thoroughly, since stable assemblies, particularly amyloid-like  $\beta$ -sheet peptide assemblies, could potentially cause negative side effects over time as a result of their systemic accumulation. Generally, the morphology, stability and overall physiological impact of synthetic nanostructures need to be closely monitored and evaluated, which is still a challenge for current methods of in vivo analysis.

In the future, further exploration of the existing toolbox of functionalities that can be reduced by glutathione, oxidized by ROS or that are labile to acidification could broaden the scope of potential precursors for intracellular self-assembly. With systems for enzyme-instructed self-assembly being prominent in recent years, the investigation of other enzymes beyond the commonly used phosphatases and proteases could not only help to diversify strategies but also contribute to a more cell-specific approach that could benefit the targeted therapy of cancer or other diseases with a characteristic dysregulation of enzyme expression. For this purpose, the study of molecular pathology is essential to lay the foundations for the design of novel enzyme-responsive materials. Moreover, including more than one bioresponsive group can increase the spatial control over the structure formation, as well as cell specificity, since multiple endogenous stimuli need to be present for assembly to occur.

Adding other bioactive components to the molecular design, such as signalling peptides<sup>48,180</sup> or small molecule drugs<sup>162</sup>, can further enhance the impact of the system on cellular processes leading to potentially synergistic therapeutic effects.

Many existing systems rely on thermodynamic control as the primary driving force to construct the intracellular architectures. Advanced methodologies involving non-equilibrium assemblies<sup>181,182</sup> coupled to cellular feedback dynamics would be highly attractive to induce reversible changes in cellular behaviour, as cell death is not always the desired outcome. From this perspective, there is also room to explore intracellular structures that boost cellular functions, possibly to address cell senescence (ageing) and environmental adaptation. The creation of such biomimetic materials that imitate reversibly formed biological supramolecular assemblies would be a milestone in synthetic biology and challenge frontiers in biomedical science.

In the upcoming years, we expect the exploration of bioresponsive materials for intracellular assembly to give rise to new sophisticated approaches to create nanostructures in complex biological environments. We hope that the design concepts presented in this Review contribute to these efforts.

Published online 1 April 2022

- Alberts, B. et al. in *Molecular Biology of the Cell* 6th edn (W. W. Norton, 2014).
- Tu, Y. et al. Mimicking the cell: bio-inspired functions of supramolecular assemblies. *Chem. Rev.* **116**, 2023–2078 (2016).
- Qi, G.-B., Gao, Y.-J., Wang, L. & Wang, H. Self-assembled peptide-based nanomaterials for biomedical imaging and therapy. *Adv. Mater.* **30**, 1703444 (2018).
- Bradshaw, D. M. & Arceci, R. J. Clinical relevance of transmembrane drug efflux as a mechanism of multidrug resistance. *J. Clin. Oncol.* **16**, 3674–3690 (1998).
- Cheng, D.-B. et al. Autocatalytic morphology transformation platform for targeted drug accumulation. *J. Am. Chem. Soc.* **141**, 4406–4411 (2019).
- Pieszka, M. et al. Controlled supramolecular assembly inside living cells by sequential multi-staged chemical reactions. *J. Am. Chem. Soc.* **142**, 15780–15789 (2020).
- A recent example of a system for a multistep reaction cascade for intracellular self-assembly.**
- Yang, P.-P. et al. Host materials transformable in tumor microenvironment for homing theranostics. *Adv. Mater.* **29**, 1605869 (2017).
- Waqas, M. et al. pH-dependent in-cell self-assembly of peptide inhibitors increases the anti-prion activity while decreasing the cytotoxicity. *Biomacromolecules* **18**, 943–950 (2017).
- Liang, G., Ren, H. & Rao, J. A biocompatible condensation reaction for controlled assembly of nanostructures in living cells. *Nat. Chem.* **2**, 54–60 (2009).
- The first example of furin-instructed self-assembly caused by enzyme-triggered macrocyclization.**
- Dong, B. et al. Reversible self-assembly of nanoprobes in live cells for dynamic intracellular pH imaging. *ACS Nano* **13**, 1421–1432 (2019).
- Cheng, Z. et al. Self-assembly of pentapeptides into morphology-adaptable nanomedicines for enhanced combinatorial chemo-photodynamic therapy. *Nano Today* **33**, 100878 (2020).
- Guo, W.-W. et al. Intracellular restructured reduced glutathione-responsive peptide nanofibers for synergistic tumor chemotherapy. *Biomacromolecules* **21**, 444–453 (2020).
- Du, W. et al. Increasing photothermal efficacy by simultaneous intra- and intermolecular fluorescence quenching. *Adv. Funct. Mater.* **30**, 1908073 (2020).
- Cheng, D.-B. et al. Endogenous reactive oxygen species-triggered morphology transformation for enhanced cooperative interaction with mitochondria. *J. Am. Chem. Soc.* **141**, 7235–7239 (2019).
- An, H.-W. et al. Bio-orthogonally deciphered binary nanoemitters for tumor diagnostics. *ACS Appl. Mater. Interfaces* **8**, 19202–19207 (2016).
- Chen, Z. et al. Exploring the condensation reaction between aromatic nitriles and amino thiols to optimize in situ nanoparticle formation for the imaging of proteases and glycosidases in cells. *Angew. Chem. Int. Ed.* **59**, 3272–3279 (2020).
- A comprehensive reactivity study of various aromatic nitriles used for the formation of aminoluciferin-based macrocycles.**
- Feng, Z. et al. Enzymatic assemblies disrupt the membrane and target endoplasmic reticulum for selective cancer cell death. *J. Am. Chem. Soc.* **140**, 9566–9573 (2018).
- Gao, Y., Shi, J., Yuan, D. & Xu, B. Imaging enzyme-triggered self-assembly of small molecules inside live cells. *Nat. Commun.* **3**, 1033 (2012).
- Kim, B. J., Fang, Y., He, H. & Xu, B. Trypsin-instructed self-assembly on endoplasmic reticulum for selectively inhibiting cancer cells. *Adv. Healthc. Mater.* **10**, 2000416 (2021).
- Wu, C., Zhang, R., Du, W., Cheng, L. & Liang, G. Alkaline phosphatase-triggered self-assembly of near-infrared nanoparticles for the enhanced photoacoustic imaging of tumors. *Nano Lett.* **18**, 7749–7754 (2018).
- Ye, D., Liang, G., Ma, M. L. & Rao, J. Controlling intracellular macrocyclization for the imaging of protease activity. *Angew. Chem. Int. Ed.* **50**, 2275–2279 (2011).
- Zheng, R. et al. Controllable self-assembly of peptide-cyanine conjugates in vivo as fine-tunable theranostics. *Angew. Chem. Int. Ed.* **60**, 7809–7819 (2021).
- Yang, Z., Liang, G., Guo, Z., Guo, Z. & Xu, B. Intracellular hydrogelation of small molecules inhibits bacterial growth. *Angew. Chem. Int. Ed.* **46**, 8216–8219 (2007).
- Hughes, M., Debnath, S., Knapp, C. W. & Ulijn, R. V. Antimicrobial properties of enzymatically triggered self-assembling aromatic peptide amphiphiles. *Biomater. Sci.* **1**, 1138–1142 (2013).
- Zou, P. et al. Recent advances: peptides and self-assembled peptide-nanosystems for antimicrobial therapy and diagnosis. *Biomater. Sci.* **8**, 4975–4996 (2020).
- Li, L.-L., An, H.-W., Peng, B., Zheng, R. & Wang, H. Self-assembled nanomaterials: design principles, the nanostructural effect, and their functional mechanisms as antimicrobial or detection agents. *Mater. Horiz.* **6**, 1794–1811 (2019).
- Mamuti, M., Zheng, R., An, H.-W. & Wang, H. In vivo self-assembled nanomedicine. *Nano Today* **36**, 101036 (2021).
- Deng, Y., Zhan, W. & Liang, G. Intracellular self-assembly of peptide conjugates for tumor imaging and therapy. *Adv. Healthc. Mater.* **10**, 2001211 (2021).
- Guo, R.-C. et al. Recent progress of therapeutic peptide based nanomaterials: from synthesis and self-assembly to cancer treatment. *Biomater. Sci.* **8**, 6175–6189 (2020).
- Hai, Z. & Liang, G. Intracellular self-assembly of nanoprobe for molecular imaging. *Adv. Biosyst.* **2**, 1800108 (2018).
- Krauss, G. in *Biochemistry of Signal Transduction and Regulation* 5th edn (Wiley, 2014).
- Ornes, S. Core concept: how nonequilibrium thermodynamics speaks to the mystery of life. *Proc. Natl Acad. Sci. USA* **114**, 423–424 (2017).
- Kaplowitz, N. The importance and regulation of hepatic glutathione. *Yale J. Biol. Med.* **54**, 497–502 (1981).
- Hanahan, D. & Weinberg, R. A. The hallmarks of cancer. *Cell* **100**, 57–70 (2000).
- Martinez-Reyes, I. & Chandel, N. S. Cancer metabolism: looking forward. *Nat. Rev. Cancer* **21**, 669–680 (2021).
- Bradley, G. & Ling, V. P-glycoprotein, multidrug resistance and tumor progression. *Cancer Metastasis Rev.* **13**, 223–233 (1994).
- Estrela, J. M., Ortega, A. & Obrador, E. Glutathione in cancer biology and therapy. *Crit. Rev. Clin. Lab. Sci.* **43**, 143–181 (2006).
- Lu, Y., Aimeetti, A. A., Langer, R. & Gu, Z. Bioresponsive materials. *Nat. Rev. Mater.* **2**, 16075 (2016).
- Yuan, Y., Kwok, R. T. K., Tang, B. Z. & Liu, B. Targeted theranostic platinum(IV) prodrug with a built-in aggregation-induced emission light-up apoptosis sensor for noninvasive early evaluation of its therapeutic responses in situ. *J. Am. Chem. Soc.* **136**, 2546–2554 (2014).
- An example of a multipurpose theranostic platform with a self-assembling aggregation-induced emission luminogen.**



40. Yuan, Y. et al. Specific light-up bioprobe with aggregation-induced emission and activatable photoactivity for the targeted and image-guided photodynamic ablation of cancer cells. *Angew. Chem. Int. Ed.* **54**, 1780–1786 (2015).
41. Shi, Y., Conde, J. & Azevedo, H. S. in *Peptides and Peptide-based Biomaterials and their Biomedical Applications* Vol. 1030 (eds Anwar, S., Care, A. & Bergquist, P. L.) 265–278 (Springer, 2017).
42. Copolovici, D. M., Langel, K., Eriste, E. & Langel, Ü. Cell-penetrating peptides: design, synthesis, and applications. *ACS Nano* **8**, 1972–1994 (2014).
43. Walrant, A., Bechara, C., Alves, I. D. & Sagan, S. Molecular partners for interaction and cell internalization of cell-penetrating peptides: how identical are they? *Nanomedicine* **7**, 133–143 (2011).
44. Richard, J. P. et al. Cellular uptake of unconjugated TAT peptide involves clathrin-dependent endocytosis and heparan sulfate receptors. *J. Biol. Chem.* **280**, 15300–15306 (2005).
45. Duchardt, F., Fotin-Mleczek, M., Schwarz, H., Fischer, R. & Brock, R. A comprehensive model for the cellular uptake of cationic cell-penetrating peptides. *Traffic* **8**, 848–866 (2007).
46. LeCher, J. C., Nowak, S. J. & McMurry, J. L. Breaking in and busting out: cell-penetrating peptides and the endosomal escape problem. *Biomol. Concepts* **8**, 131–141 (2017).
47. Caswell, P. T., Vadrevu, S. & Norman, J. C. Integrins: masters and slaves of endocytic transport. *Nat. Rev. Mol. Cell Biol.* **10**, 843–853 (2009).
48. An, H.-W. et al. A tumour-selective cascade activatable self-detained system for drug delivery and cancer imaging. *Nat. Commun.* **10**, 4861 (2019).  
**A fascinating example of a peptide-based system that can induce the expression of caspases 3 and 7 in tumour cells and subsequently be cleaved by them.**
49. Fang, J., Nakamura, H. & Maeda, H. The EPR effect: unique features of tumor blood vessels for drug delivery, factors involved, and limitations and augmentation of the effect. *Adv. Drug Deliv. Rev.* **63**, 136–151 (2011).
50. Chen, Z., Chen, M., Zhou, K. & Rao, J. Pre-targeted imaging of protease activity through in situ assembly of nanoparticles. *Angew. Chem. Int. Ed.* **59**, 7864–7870 (2020).  
**A sophisticated approach to image the in vivo activity of caspases 3 and 7 using a combination of intracellular self-assembly and biorthogonal click chemistry.**
51. Li, J. et al. Enzyme-instructed intracellular molecular self-assembly to boost activity of cisplatin against drug-resistant ovarian cancer cells. *Angew. Chem. Int. Ed.* **54**, 13307–13311 (2015).
52. Ellis, R. J. Macromolecular crowding: an important but neglected aspect of the intracellular environment. *Curr. Opin. Struct. Biol.* **11**, 114–119 (2001).
53. Feng, Z. et al. Artificial intracellular filaments. *Cell Rep. Phys. Sci.* **1**, 100085 (2020).  
**An in-depth study of the cell biological effects of phosphatase-instructed assembly formation.**
54. Hansen, R. E., Roth, D. & Winther, J. R. Quantifying the global cellular thiol–disulfide status. *Proc. Natl Acad. Sci. USA* **106**, 422–427 (2009).
55. Estrela, J. M., Obrador, E., Navarro, J., De La Vega, M. C. L. & Pellicer, J. A. Elimination of Ehrlich tumours by ATP-induced growth inhibition, glutathione depletion and X-rays. *Nat. Med.* **1**, 84–88 (1995).
56. Veal, E. A., Day, A. M. & Morgan, B. A. Hydrogen peroxide sensing and signaling. *Mol. Cell* **26**, 1–14 (2007).
57. Wang, H. et al. Integrating enzymatic self-assembly and mitochondria targeting for selectively killing cancer cells without acquired drug resistance. *J. Am. Chem. Soc.* **138**, 16046–16055 (2016).
58. Qiao, S.-L., Ma, Y., Wang, Y., Lin, Y.-X. & Wang, H. General approach of stimuli-induced aggregation for monitoring tumor therapy. *ACS Nano* **11**, 7301–7311 (2017).  
**A comprehensive study of using various endogenous triggers for polymer self-assembly inside living cells.**
59. Yuan, Y. et al. Casp3/7-instructed intracellular aggregation of Fe<sub>3</sub>O<sub>4</sub> nanoparticles enhances T<sub>2</sub> MR imaging of tumor apoptosis. *Nano Lett.* **16**, 2686–2691 (2016).
60. Ding, Z. et al. Furin-controlled Fe<sub>3</sub>O<sub>4</sub> nanoparticle aggregation and <sup>19</sup>F signal “turn-on” for precise MR imaging of tumors. *Adv. Funct. Mater.* **29**, 1903860 (2019).
61. Chen, J. et al. Furin-instructed intracellular gold nanoparticle aggregation for tumor photothermal therapy. *Adv. Funct. Mater.* **30**, 2001566 (2020).
62. Levin, A. et al. Biomimetic peptide self-assembly for functional materials. *Nat. Rev. Chem.* **4**, 615–634 (2020).
63. Wang, H., Feng, Z. & Xu, B. Assemblies of peptides in a complex environment and their applications. *Angew. Chem. Int. Ed.* **58**, 10423–10432 (2019).
64. Hendricks, M. P., Sato, K., Palmer, L. C. & Stupp, S. I. Supramolecular assembly of peptide amphiphiles. *Acc. Chem. Res.* **50**, 2440–2448 (2017).
65. Bakshi, R. et al. A chemotactic functional scaffold with VEGF-releasing peptide amphiphiles facilitates bone regeneration by BMP-2 in a large-scale rodent cranial defect model. *Plast. Reconstr. Surg.* **147**, 386–397 (2020).
66. Zhou, S. et al. Bioactive peptide amphiphile nanofiber gels enhance burn wound healing. *Burns* **45**, 1112–1121 (2019).
67. Tanaka, A. et al. Cancer cell death induced by the intracellular self-assembly of an enzyme-responsive supramolecular gelator. *J. Am. Chem. Soc.* **137**, 770–775 (2015).
68. Yamamoto, S. et al. Microenvironment pH-induced selective cell death for potential cancer therapy using nanofibrous self-assembly of a peptide amphiphile. *Biomacromolecules* **22**, 2524–2531 (2021).
69. He, P.-P., Li, X.-D., Wang, L. & Wang, H. Bispyrene-based self-assembled nanomaterials: in vivo self-assembly, transformation, and biomedical effects. *Acc. Chem. Res.* **52**, 367–378 (2019).
70. Wang, L. et al. Supramolecular nano-aggregates based on bis(pyrene) derivatives for lysosome-targeted cell imaging. *J. Phys. Chem. C* **117**, 26811–26820 (2013).
71. Wang, D. et al. Highly efficient photosensitizers with far-red/near-infrared aggregation-induced emission for in vitro and in vivo cancer theranostics. *Adv. Mater.* **30**, 1802105 (2018).
72. Zheng, Z. et al. Bright near-infrared aggregation-induced emission luminogens with strong two-photon absorption, excellent organelle specificity, and efficient photodynamic therapy potential. *ACS Nano* **2018**, 8145–8159 (2018).
73. Niu, G. et al. Highly photostable two-photon NIR AIEgens with tunable organelle specificity and deep tissue penetration. *Biomaterials* **208**, 8145–8159 (2019).
74. Zhang, T. et al. In situ monitoring apoptosis process by a self-reporting photosensitizer. *J. Am. Chem. Soc.* **141**, 5612–5616 (2019).
75. Yuan, Y. & Liang, G. A biocompatible, highly efficient click reaction and its applications. *Org. Biomol. Chem.* **12**, 865–871 (2014).
76. Kuang, Y. & Xu, B. Disruption of the dynamics of microtubules and selective inhibition of glioblastoma cells by nanofibers of small hydrophobic molecules. *Angew. Chem. Int. Ed.* **52**, 6944–6948 (2013).
77. Jin, S. et al. Spatiotemporal self-assembly of peptides dictates cancer-selective toxicity. *Biomacromolecules* **21**, 4806–4813 (2020).
78. Jeena, M. T. et al. Heterochiral assembly of amphiphilic peptides inside the mitochondria for supramolecular cancer therapeutics. *ACS Nano* **13**, 11022–11033 (2019).
79. Jeena, M. T. et al. Mitochondria localization induced self-assembly of peptide amphiphiles for cellular dysfunction. *Nat. Commun.* **8**, 26 (2017).  
**An interesting approach to organelle-specific self-assembly caused by targeting-driven local accumulation.**
80. Ng, D. Y. W. et al. Directing intracellular supramolecular assembly with N-heteroaromatic quaterthiophene analogues. *Nat. Commun.* **8**, 1850 (2017).  
**An in-depth study of the subcellular distribution and self-assembly of oligo thiophene conjugates.**
81. Wang, H., Feng, Z., Tan, W. & Xu, B. Assemblies of D-peptides for targeting cell nucleolus. *Bioconjugate Chem.* **30**, 2528–2532 (2019).
82. Webb, B. A., Chimenti, M., Jacobson, M. P. & Barber, D. L. Dysregulated pH: a perfect storm for cancer progression. *Nat. Rev. Cancer* **11**, 671–677 (2011).
83. Casey, J. R., Grinstein, S. & Orlowski, J. Sensors and regulators of intracellular pH. *Nat. Rev. Mol. Cell Biol.* **11**, 50–61 (2009).
84. Li, M. et al. Proline isomerization-regulated tumor microenvironment-adaptable self-assembly of peptides for enhanced therapeutic efficacy. *Nano Lett.* **19**, 7965–7976 (2019).  
**An example of a pH-responsive morphology-adaptable peptide used for in vivo self-assembly in tumour cells.**
85. Cody, S. H. et al. Intracellular pH mapping with SNARF-1 and confocal microscopy. I: A quantitative technique for living tissue and isolated cells. *Micron* **24**, 573–580 (1993).
86. Cote, Y. et al. Mechanism of the pH-controlled self-assembly of nanofibers from peptide amphiphiles. *J. Phys. Chem. C* **118**, 16272–16278 (2014).
87. Shaw, P. E. Peptidyl-prolyl isomerases: a new twist to transcription. *EMBO Rep.* **3**, 521–526 (2002).
88. Sies, H. Glutathione and its role in cellular functions. *Free Radic. Biol. Med.* **27**, 916–921 (1999).
89. Lu, S. C. Regulation of hepatic glutathione synthesis: current concepts and controversies. *FASEB J.* **13**, 1169–1183 (1999).
90. Carretero, J. et al. Growth-associated changes in glutathione content correlate with liver metastatic activity of B16 melanoma cells. *Clin. Exp. Metastasis* **17**, 567–574 (1999).
91. Gamcsik, M. P., Kasibhatla, M. S., Teeter, S. D. & Colvin, O. M. Glutathione levels in human tumors. *Biomarkers* **17**, 671–691 (2012).
92. Depelle, P., Cuq, P., Passagne, I., Evraud, A. & Vian, L. Combined effects of GSTP1 and MRP1 in melanoma drug resistance. *Br. J. Cancer* **93**, 216–223 (2005).
93. Quinn, J. F., Whittaker, M. R. & Davis, T. P. Glutathione responsive polymers and their application in drug delivery systems. *Polym. Chem.* **8**, 97–126 (2016).
94. Zhan, J., Cai, Y., He, S., Wang, L. & Yang, Z. Tandem molecular self-assembly in liver cancer cells. *Angew. Chem. Int. Ed.* **57**, 1813–1816 (2018).
95. Spooner, R. & Yilmaz, Ö. The role of reactive-oxygen-species in microbial persistence and inflammation. *Int. J. Mol. Sci.* **12**, 334–352 (2011).
96. Geiszt, M. & Leto, T. L. The Nox family of NAD(P)H oxidases: host defense and beyond. *J. Biol. Chem.* **279**, 51715–51718 (2004).
97. D’Autréaux, B. & Toledano, M. B. ROS as signalling molecules: mechanisms that generate specificity in ROS homeostasis. *Nat. Rev. Mol. Cell Biol.* **8**, 813–824 (2007).
98. Houstis, N., Rosen, E. D. & Lander, E. S. Reactive oxygen species have a causal role in multiple forms of insulin resistance. *Nature* **440**, 944–948 (2006).
99. Touyz, R. M. & Schiffrin, E. L. Reactive oxygen species in vascular biology: implications in hypertension. *Histochem. Cell Biol.* **122**, 339–352 (2004).
100. Behrend, L., Henderson, G. & Zwacka, R. M. Reactive oxygen species in oncogenic transformation. *Biochem. Soc. Trans.* **31**, 1441–1444 (2003).
101. Wu, W.-S. The signaling mechanism of ROS in tumor progression. *Cancer Metastasis Rev.* **25**, 695–705 (2006).
102. Trachootham, D., Alexandre, J. & Huang, P. Targeting cancer cells by ROS-mediated mechanisms: a radical therapeutic approach? *Nat. Rev. Drug Discov.* **8**, 579–591 (2009).
103. Dickinson, B. C. & Chang, C. J. Chemistry and biology of reactive oxygen species in signaling or stress responses. *Nat. Chem. Biol.* **7**, 504–511 (2011).
104. Liu, B. & Thayumanavan, S. Mechanistic investigation on oxidative degradation of ROS-responsive thioacetal/thioether moieties and their implications. *Cell Rep. Phys. Sci.* **1**, 100271 (2020).
105. Li, L.-L. et al. Intracellular construction of topology-controlled polypeptide nanostructures with diverse biological functions. *Nat. Commun.* **8**, 1276 (2017).
106. He, H., Guo, J., Lin, X. & Xu, B. Enzyme-instructed assemblies enable mitochondria localization of histone H2B in cancer cells. *Angew. Chem. Int. Ed.* **59**, 9330–9334 (2020).
107. López-Otin, C. & Bond, J. S. Proteases: multifunctional enzymes in life and disease. *J. Biol. Chem.* **283**, 30435–30437 (2008).
108. Molloy, S. S., Bresnahan, P. A., Leppla, S. H., Klimpel, K. R. & Thomas, G. Human furin is a calcium-dependent serine endoprotease that recognizes the sequence Arg-X-X-Arg and efficiently cleaves anthrax toxin protective antigen. *J. Biol. Chem.* **267**, 16396–16402 (1992).
109. Jaaks, P. & Bernasconi, M. The proprotein convertase furin in tumour progression. *Int. J. Cancer* **141**, 654–663 (2017).
110. Bassi, D. E., Fu, J., de Cicco, R. L. & Klein-Szanto, A. J. P. Proprotein convertases: “master switches” in the regulation of tumor growth and progression. *Mol. Cell. Oncol.* **44**, 151–161 (2005).

111. Ozden, S. et al. Inhibition of Chikungunya virus infection in cultured human muscle cells by furin inhibitors. *J. Biol. Chem.* **283**, 21899–21908 (2008).
112. Bestle, D. et al. TMPRSS2 and furin are both essential for proteolytic activation of SARS-CoV-2 in human airway cells. *Life Sci. Alliance* **3**, e202000786 (2020).
113. Dragulescu-Andrasi, A., Kothapalli, S.-R., Tikhomirov, G. A., Rao, J. & Gambhir, S. S. Activatable oligomerizable imaging agents for photoacoustic imaging of furin-like activity in living subjects. *J. Am. Chem. Soc.* **135**, 11015–11022 (2013). **An example of the in vivo application of a furin-responsive macrocyclization precursor for photoacoustic cancer imaging.**
114. Liu, Y. et al. Enzyme-controlled intracellular self-assembly of <sup>18</sup>F nanoparticles for enhanced microPET imaging of tumor. *Theranostics* **5**, 1058–1067 (2015).
115. Miao, Q. et al. Intracellular self-assembly of nanoparticles for enhancing cell uptake. *Chem. Commun.* **48**, 9738–9740 (2012).
116. Yuan, Y. et al. Furin-mediated self-assembly of olsalazine nanoparticles for targeted Raman imaging of tumors. *Angew. Chem. Int. Ed.* **60**, 3923–3927 (2020).
117. Yuan, Y. et al. Furin-mediated intracellular self-assembly of olsalazine nanoparticles for enhanced magnetic resonance imaging and tumour therapy. *Nat. Mater.* **18**, 1376–1383 (2019).
118. Yuan, Y. et al. Intracellular self-assembly of Taxol nanoparticles for overcoming multidrug resistance. *Angew. Chem. Int. Ed.* **54**, 9700–9704 (2015).
119. Li, J. & Yuan, J. Caspases in apoptosis and beyond. *Oncogene* **27**, 6194–6206 (2008).
120. Riedl, S. J. & Shi, Y. Molecular mechanisms of caspase regulation during apoptosis. *Nat. Rev. Mol. Cell Biol.* **5**, 897–907 (2004).
121. McComb, S. et al. Efficient apoptosis requires feedback amplification of upstream apoptotic signals by effector caspase-3 or -7. *Sci. Adv.* **5**, eaau9433 (2019).
122. Walsh, J. G. et al. Executioner caspase-3 and caspase-7 are functionally distinct proteases. *Proc. Natl Acad. Sci. USA* **105**, 12815–12819 (2008).
123. Shi, H. et al. Real-time monitoring of cell apoptosis and drug screening using fluorescent light-up probe with aggregation-induced emission characteristics. *J. Am. Chem. Soc.* **134**, 17972–17981 (2012).
124. Huang, R. et al. Multifunctional fluorescent probe for sequential detections of glutathione and caspase-3 in vitro and in cells. *Anal. Chem.* **85**, 6203–6207 (2013).
125. Ye, D. et al. Bioorthogonal cyclization-mediated in situ self-assembly of small-molecule probes for imaging caspase activity in vivo. *Nat. Chem.* **6**, 519–526 (2014).
126. Tong, H. et al. Protein detection and quantitation by tetraphenylethene-based fluorescent probes with aggregation-induced emission characteristics. *J. Phys. Chem. B* **111**, 11817–11823 (2007).
127. Niu, G. et al. AIE luminogens as fluorescent bioprobes. *Trends Anal. Chem.* **123**, 115769 (2020).
128. Sharma, S. K., Straub, C. & Zawal, L. Development of peptidomimetics targeting IAPs. *Int. J. Pept. Res. Ther.* **12**, 21–32 (2006).
129. Deveraux, Q. L., Takahashi, R., Salvesen, G. S. & Reed, J. C. X-linked IAP is a direct inhibitor of cell-death proteases. *Nature* **388**, 300–304 (1997).
130. Blanco, G. & Blanco, A. in *Medical Biochemistry* (Academic, 2017).
131. Light, A. & Janska, H. Enterokinase (enteropeptidase): comparative aspects. *Trends Biochem. Sci.* **14**, 110–112 (1989).
132. Kitamoto, Y., Yuan, X., Wu, Q., McCourt, D. W. & Sadler, J. E. Enterokinase, the initiator of intestinal digestion, is a mosaic protease composed of a distinctive assortment of domains. *Proc. Natl Acad. Sci. USA* **91**, 7588–7592 (1994).
133. He, H. et al. Enzymatic cleavage of branched peptides for targeting mitochondria. *J. Am. Chem. Soc.* **140**, 1215–1218 (2018).
134. He, H. et al. Enzymatic noncovalent synthesis for mitochondrial genetic engineering of cancer cells. *Cell Rep. Phys. Sci.* **1**, 100270 (2020).
135. He, H., Lin, X., Guo, J., Wang, J. & Xu, B. Perimitochondrial enzymatic self-assembly for selective targeting the mitochondria of cancer cells. *ACS Nano* **14**, 6947–6955 (2020).
136. Luengo-Gil, G. et al. Antithrombin controls tumor migration, invasion and angiogenesis by inhibition of enteropeptidase. *Sci. Rep.* **6**, 27544 (2016).
137. Moilanen, M. et al. Tumor-associated trypsinogen-2 (trypsinogen-2) activates procollagenases (MMP-1, -8, -13) and stromelysin-1 (MMP-3) and degrades type I collagen. *Biochemistry* **42**, 5414–5420 (2003).
138. Yamamoto, H. et al. Association of trypsin expression with tumour progression and matrixlysin expression in human colorectal cancer. *J. Pathol.* **199**, 176–184 (2003).
139. Soreide, K., Janssen, E. A., Körner, H. & Baak, J. Trypsin in colorectal cancer: molecular biological mechanisms of proliferation, invasion, and metastasis. *J. Pathol.* **209**, 147–156 (2006).
140. Miyata, S. et al. Expression of trypsin in human cancer cell lines and cancer tissues and its tight binding to soluble form of Alzheimer amyloid precursor protein in culture. *J. Biochem.* **125**, 1067–1076 (1999).
141. Hockla, A. et al. PRSS3/mesotrypsin is a therapeutic target for metastatic prostate cancer. *Mol. Cancer Res.* **10**, 1555–1566 (2012).
142. Koivunen, E. et al. Tumor-associated trypsin participates in cancer cell-mediated degradation of extracellular matrix. *Cancer Res.* **51**, 2107–2112 (1991).
143. Sorsa, T. et al. Activation of type IV procollagenases by human tumor-associated trypsin-2. *J. Biol. Chem.* **272**, 21067–21074 (1997).
144. Vilen, S.-T. et al. Intracellular co-localization of trypsin-2 and matrix metalloproteinase-9: possible proteolytic cascade of trypsin-2, MMP-9 and enterokinase in carcinoma. *Exp. Cell Res.* **314**, 914–926 (2008).
145. Podgorski, I. & Sloane, B. F. Cathepsin B and its role(s) in cancer progression. *Biochem. Soc. Symp.* **70**, 263–276 (2003).
146. Campo, E. et al. Cathepsin B expression in colorectal carcinomas correlates with tumor progression and shortened patient survival. *Am. J. Pathol.* **145**, 301–309 (1994).
147. Bengsch, F. et al. Cell type-dependent pathogenic functions of overexpressed human cathepsin B in murine breast cancer progression. *Oncogene* **33**, 4474–4484 (2014).
148. Malla, R. R. et al. Cathepsin B and uPAR knockdown inhibits tumor-induced angiogenesis by modulating VEGF expression in glioma. *Cancer Gene Ther.* **18**, 419–434 (2011).
149. Dheer, D., Nicolas, J. & Shankar, R. Cathepsin-sensitive nanoscale drug delivery systems for cancer therapy and other diseases. *Adv. Drug Deliv. Rev.* **151–152**, 130–151 (2019).
150. Quantin, B., Murphy, G. & Breathnach, R. Pump-1 cDNA codes for a protein with characteristics similar to those of classical collagenase family members. *Biochemistry* **28**, 5327–5334 (1989).
151. Polette, M., Nawrocki-Raby, B., Gilles, C., Clavel, C. & Birembaut, P. Tumour invasion and matrix metalloproteinases. *Crit. Rev. Oncol. Hematol.* **49**, 179–186 (2004).
152. Xu, D. et al. Identification of new ATG4B inhibitors based on a novel high-throughput screening platform. *SLAS Discov.* **22**, 338–347 (2016).
153. Guo, J. Y., Xia, B. & White, E. Autophagy-mediated tumor promotion. *Cell* **155**, 1216–1219 (2013).
154. Mathew, R., Karantza-Wadsworth, V. & White, E. Role of autophagy in cancer. *Nat. Rev. Cancer* **7**, 961–967 (2007).
155. Nixon, R. A. The role of autophagy in neurodegenerative disease. *Nat. Med.* **19**, 983–997 (2013).
156. Fujita, N. et al. An Atg4B mutant hampers the lipidation of LC3 paralogs and causes defects in autophagosomal closure. *Mol. Biol. Cell* **19**, 4651–4659 (2008).
157. Lin, Y.-X. et al. An in situ intracellular self-assembly strategy for quantitatively and temporally monitoring autophagy. *ACS Nano* **11**, 1826–1839 (2017).
158. Graves, J. D. & Krebs, E. G. Protein phosphorylation and signal transduction. *Pharmacol. Ther.* **82**, 111–121 (1999).
159. Li, X., Wilmanns, M., Thornton, J. & Köhn, M. Elucidating human phosphatase-substrate networks. *Sci. Signal.* **6**, rs10 (2013).
160. Lin, C.-W., Sasaki, M., Orcutt, M. L., Miyayama, H. & Singer, R. M. Plasma membrane localization of alkaline phosphatase in HeLa cells. *J. Histochem. Cytochem.* **24**, 659–667 (1976).
161. Frangioni, J. V., Beahm, P. H., Shifrin, V., Jost, C. A. & Neel, B. G. The nontransmembrane tyrosine phosphatase PTP-1B localizes to the endoplasmic reticulum via its 35 amino acid C-terminal sequence. *Cell* **68**, 545–560 (1992).
162. Gao, Y. et al. Enzyme-instructed molecular self-assembly confers nanofibers and a supramolecular hydrogel of Taxol derivative. *J. Am. Chem. Soc.* **131**, 13576–13577 (2009).
163. Gao, Y. et al. Probing nanoscale self-assembly of nonfluorescent small molecules inside live mammalian cells. *ACS Nano* **7**, 9055–9063 (2013).
164. Gao, Y. et al. Imaging self-assembly dependent spatial distribution of small molecules in a cellular environment. *Langmuir* **29**, 15191–15200 (2013). **A study of the influence of a fluorescent unit on assembly behaviour, cellular distribution and impact.**
165. Humphries, G. M. & Lovejoy, J. P. Dansyl lysine: a structure-selective fluorescent membrane stain? *Biophys. J.* **42**, 307–310 (1983).
166. Feng, Z., Wang, H. & Xu, B. Instructed assembly of peptides for intracellular enzyme sequestration. *J. Am. Chem. Soc.* **140**, 16433–16437 (2018). **An example of combining a phosphatase-sensitive precursor with a COX2 enzyme substrate for organelle-specific assembly and enzyme sequestration.**
167. Tan, W. et al. Enzymatic assemblies of thiophosphopeptides instantly target Golgi apparatus and selectively kill cancer cells. *Angew. Chem. Int. Ed.* **60**, 12796–12801 (2021).
168. Dimri, G. P. et al. A biomarker that identifies senescent human cells in culture and in aging skin in vivo. *Proc. Natl Acad. Sci. USA* **92**, 9363–9367 (1995).
169. Chang, J. et al. Clearance of senescent cells by ABT263 rejuvenates aged hematopoietic stem cells in mice. *Nat. Med.* **22**, 78–83 (2016).
170. Campisi, J. Senescent cells, tumor suppression, and organismal aging: good citizens, bad neighbors. *Cell* **120**, 513–522 (2005).
171. Xu, T. et al.  $\beta$ -Galactosidase instructed supramolecular hydrogelation for selective identification and removal of senescent cells. *Chem. Commun.* **55**, 7175–7178 (2019).
172. Xu, G., Zhang, W., Ma, M. K. & McLeod, H. L. Human carboxylesterase 2 is commonly expressed in tumor tissue and is correlated with activation of irinotecan. *Clin. Cancer Res.* **8**, 2605–2611 (2002).
173. Yang, Z. M., Xu, K. M., Guo, Z. F., Guo, Z. H. & Xu, B. Intracellular enzymatic formation of nanofibers results in hydrogelation and regulated cell death. *Adv. Mater.* **19**, 3152–3156 (2007).
174. Zhou, J., Du, X., Li, J., Yamagata, N. & Xu, B. Taurine boosts cellular uptake of small D-peptides for enzyme-instructed intracellular molecular self-assembly. *J. Am. Chem. Soc.* **137**, 10040–10043 (2015).
175. Li, J. et al. Selectively inducing cancer cell death by intracellular enzyme-instructed self-assembly (EISA) of dipeptide derivatives. *Adv. Healthc. Mater.* **6**, 1601400 (2017).
176. Li, J. et al. Kinetic analysis of nanostructures formed by enzyme-instructed intracellular assemblies against cancer cells. *ACS Nano* **12**, 3804–3815 (2018).
177. Lorand, L. & Graham, R. M. Transglutaminases: crosslinking enzymes with pleiotropic functions. *Nat. Rev. Mol. Cell Biol.* **4**, 140–156 (2003).
178. Zhang, M. et al. Directly observing intracellular nanoparticle formation with nanocomputed tomography. *Sci. Adv.* **6**, eaab3190 (2020).
179. Yang, J., An, H.-W. & Wang, H. Self-assembled peptide drug delivery systems. *ACS Appl. Bio Mater.* **4**, 24–46 (2021).
180. He, H., Liu, S., Wu, D. & Xu, B. Enzymatically formed peptide assemblies sequester proteins and relocate inhibitors to selectively kill cancer cells. *Angew. Chem. Int. Ed.* **59**, 16445–16450 (2020).
181. Debnath, S., Roy, S. & Ulijn, R. V. Peptide nanofibers with dynamic instability through nonequilibrium biocatalytic assembly. *J. Am. Chem. Soc.* **135**, 16789–16792 (2013).
182. Boekhoven, J., Hendriksen, W. E., Koper, G. J. M., Eelkema, R. & van Esch, J. H. Transient assembly of active materials fueled by a chemical reaction. *Science* **349**, 1075–1079 (2015).
183. Hai, Z. et al. Smart dual quenching strategy enhances the detection sensitivity of intracellular furin. *Anal. Chem.* **90**, 1520–1524 (2018).
184. Yao, Q. et al. Synergistic enzymatic and bioorthogonal reactions for selective prodrug activation in living systems. *Nat. Commun.* **9**, 5032 (2018).
185. Yang, S. et al. Enzyme-triggered self-assembly of gold nanoparticles for enhanced retention effects and photothermal therapy of prostate cancer. *Chem. Commun.* **54**, 9841–9844 (2018).



186. Wang, J. et al. Cell-compatible nanoprobes for imaging intracellular phosphatase activities. *ChemBioChem* **20**, 526–531 (2019).
187. Tang, W., Yang, J., Zhao, Z., Lian, Z. & Liang, G. Intracellular coassembly boosts the anti-inflammation capacity of dexamethasone. *Nanoscale* **9**, 17717–17721 (2017).
188. Huang, A. et al. In situ enzymatic formation of supramolecular nanofibers for efficiently killing cancer cells. *RSC Adv.* **6**, 32519–32522 (2016).
189. Dong, L., Miao, Q., Hai, Z., Yuan, Y. & Liang, G. Enzymatic hydrogelation-induced fluorescence turn-off for sensing alkaline phosphatase in vitro and in living cells. *Anal. Chem.* **87**, 6475–6478 (2015).

190. Hai, Z. et al.  $\gamma$ -Glutamyltranspeptidase-triggered intracellular gadolinium nanoparticle formation enhances the  $T_2$ -weighted MR contrast of tumor. *Nano Lett.* **19**, 2428–2433 (2019).

#### Acknowledgements

The authors acknowledge funding by the Max Planck-Bristol Centre for Minimal Biology and the Max Planck Society. This work was supported by the Max Planck Graduate Center (MPGC) with the Johannes Gutenberg University Mainz.

#### Author contributions

S.C. researched data for the article, contributed to discussion of content and wrote the article. D.Y.W.N. and T.W. edited the manuscript and contributed substantially to discussion of

the content. All authors reviewed the manuscript before submission.

#### Competing interests

The authors declare no competing interests.

#### Peer review information

*Nature Reviews Chemistry* thanks J. Shen (who co-reviewed with R. Liu) and the other, anonymous, reviewers for their contribution to the peer review of this work.

#### Publisher's note

Springer Nature remains neutral with regard to jurisdictional claims in published maps and institutional affiliations.

© Springer Nature Limited 2022